















# Linking the oxygen-17 compositions of water and carbonate reference materials using infrared absorption spectroscopy of carbon dioxide

J. Chaillot <sup>\*</sup>(1,2)  , S. Kassi <sup>(2)</sup>  , T. Clauzel <sup>(1)</sup>  , M. Pesnin <sup>(1)</sup>  , M. Casado <sup>(1)</sup>  ,  
A. Landais <sup>(1)</sup>  , M. Daëron <sup>(1)</sup>  

*\*corresponding author*

(1) Laboratoire des Sciences du Climat et de l'Environnement, LSCE/IPSL, CEA-CNRS-UVSQ, Université Paris-Saclay, France

(2) Laboratoire Interdisciplinaire de Physique, Université Grenoble Alpes, CNRS, Grenoble, France

---

Joint measurements of the  $^{18}\text{O}/^{16}\text{O}$  and  $^{17}\text{O}/^{16}\text{O}$  ratios of carbonate minerals and waters are increasingly used to investigate various geochemical, physical and biological processes. Diverse analytical methods, each of them technically challenging in one way or another, have been developed or refined in recent years to measure oxygen-17 anomalies ( $\Delta^{17}\text{O}$ ) with instrumental precisions of 10 ppm or better. Constraining the triple oxygen isotope compositions of the international carbonate reference materials (RM), relative to each other and relative to the primary VSMOW-SLAP scale, is a critical underpinning of all these methods. For now, however, substantial systematic discrepancies persist between different groups and methods, even after all measurements are nominally standardized to VSMOW-SLAP.

Here we take advantage of VCOF-CRDS, a novel spectroscopic method combining the ease and simplicity of near-infrared absorption measurements in pure  $\text{CO}_2$  with metrological performance competitive with state-of-the-art IRMS techniques, to precisely characterize, based on previously reported equilibrium fractionation factors between water and  $\text{CO}_2$ , the relative triple oxygen isotope compositions of international water standards (VSMOW2, SLAP2, GRESP) and  $\text{CO}_2$  produced by phosphoric acid reaction of carbonate standards (NBS18, NBS19, IAEA603, IAEA610, IAEA611, IAEA612). The robustness of our results derives from the demonstrated linearity of our measurements (RMSE  $\approx$  1 ppm), but also from the fact that, when equilibrated with or converted to  $\text{CO}_2$ , both water and carbonate RMs yield analytes with closely comparable oxygen-18 compositions. In light of these observations, we revisit potential causes of the large inter-laboratory discrepancies reported so far. Collectively reconciling the different types of measurements constraining the relative  $^{17}\text{O}/^{16}\text{O}$  ratios of the two standards most often used to normalize carbonate analyses (NBS18, IAEA603) is a matter of high priority.

---

In press, *Chemical Geology*

# 1 Introduction

As originally postulated by H. Craig [1], the stable isotope ratios  $^{18}\text{O}/^{16}\text{O}$  and  $^{17}\text{O}/^{16}\text{O}$  in most natural oxygen-bearing materials on Earth may be described, to the first order, as following a simple power law linking any two phases A and B:

$$\frac{[^{17}\text{O}/^{16}\text{O}]_A}{[^{17}\text{O}/^{16}\text{O}]_B} = \left( \frac{[^{18}\text{O}/^{16}\text{O}]_A}{[^{18}\text{O}/^{16}\text{O}]_B} \right)^{\lambda \approx 1/2} \quad (1)$$

Leaving aside large deviations from this power law, such as found in the Earth's stratosphere and in extra-terrestrial materials, smaller departures corresponding to  $^{17}\text{O}/^{16}\text{O}$  "anomalies" up to a few tenths of permil are commonplace, and may be used to gain additional information beyond that obtained from  $^{18}\text{O}/^{16}\text{O}$  alone [2].

In carbonate minerals, these  $^{17}\text{O}$  anomalies are a potentially crucial source of information on past climates, paleo-hydrology, diagenesis, biocalcification processes, and the long-term oxygen and carbon cycles [3–9]. However, measuring them with the required precision and accuracy, whether directly from the mineral phase or in  $\text{CO}_2$  produced by phosphoric acid reaction of carbonate minerals, remains challenging. Even state-of-the-art isotope-ratio mass spectrometric (IRMS) techniques are notoriously unable to resolve  $^{16}\text{O}^{13}\text{C}^{16}\text{O}$  (with a mass of 44.9932 Da) from  $^{16}\text{O}^{12}\text{C}^{17}\text{O}$  (44.9940 Da) with sufficient precision, so that various methods have been designed to transfer the triple oxygen signature of carbon dioxide to molecular oxygen.

The most successful IRMS approaches so far have been (1) quantitative extraction of oxygen from  $\text{CO}_2$  or carbonate samples by high-temperature fluorination [10–12]; (2) quantitative conversion of  $\text{CO}_2$  or carbonate samples to methane and water, followed by conversion of  $\text{H}_2\text{O}$  to  $\text{O}_2$  by fluorination [3, 13, 14] (3) controlled oxygen exchange with a finite amount of metal oxide [15–18], water [19], or molecular oxygen [20, 21]. Other methods exist [22, 23] but for typical "small" sample sizes (10–100  $\mu\text{mol}$ ) they do not currently achieve the analytical precision (0.01 ‰ or better) attainable with the techniques listed above.

Molecular absorption spectroscopy is well suited to more direct measurements of triple oxygen isotopes in  $\text{CO}_2$ , because the roto-vibrational modes of excitation responsible for absorption in the infra-red spectrum do not depend on total isotopologue mass but on the distribution of mass within each isotopologue. As a result,  $^{16}\text{O}^{13}\text{C}^{16}\text{O}$  and  $^{16}\text{O}^{12}\text{C}^{17}\text{O}$  (hereafter noted 636 and 627, following the spectroscopic shorthand described in section 2.1) have distinct absorption spectra and one may precisely quantify the relative abundances of 626, 627 and 628 isotopologues by targeting spectrally isolated absorption peaks [24]. Optical techniques have long struggled to reach the metrological precision and linearity of IRMS methods, but recent developments have closed the gap, with measurements of rare  $\text{CO}_2$  isotopologues, including doubly-substituted species such as 638, achieving instrumental precision comparable to state-of-the-art IRMS [25–28].

Analyses of water and  $\text{O}_2$  are standardized relative to the Vienna Standard Mean Ocean Water - Standard Light Antarctic Precipitation (VSMOW-SLAP) scale. Carbonate  $\delta^{13}\text{C}$  and  $\delta^{18}\text{O}$  values are canonically tied to the Vienna Pee Dee Belemnite (VPDB) scale, which by consensus is tied to VSMOW by the following equation [29, 30]. This secondary oxygen-18 scale tied to carbonate reference materials, which may seem mathematically superfluous, makes it possible to standardize carbonate analyses following the widely-accepted principle of identical treatment of samples and standards [31].

$$[^{18}\text{O}/^{16}\text{O}]_{\text{VPDB}} = 1.03092 \cdot [^{18}\text{O}/^{16}\text{O}]_{\text{VSMOW}} \quad (2)$$

There is however no consensus on an similar relationship linking  $[^{17}\text{O}/^{16}\text{O}]_{\text{VPDB}}$  and  $[^{17}\text{O}/^{16}\text{O}]_{\text{VSMOW}}$  or, equivalently, on the nominal  $^{17}\text{O}/^{16}\text{O}$  ratio in primary carbonate reference materials such as NBS18 or IAEA603. Several estimates have been put forward in the past decade [3, 12, 14, 32–34], with large systematic differences across groups and methods, including smaller apparent discrepancies in the relative oxygen-17 compositions of carbonate standards (cf Table 5 of *Sharp & Wostbrock* [35]).

The oxygen-18 variability in carbonate minerals found on Earth reflect that of natural waters, further modified by physical and chemical processes which form the basis of oxygen-18 thermometry, one of the oldest and most widely used geochemical proxies. A critical underpinning of triple oxygen isotope studies of carbonate minerals is thus to tie, as accurately as possible, the VPDB scale to the VSMOW-SLAP scale in  $^{16}\text{O}/^{17}\text{O}/^{18}\text{O}$  space by constraining the  $^{17}\text{O}$  compositions, relative to VSMOW-SLAP, of at least two carbonate standards with sufficiently different  $^{18}\text{O}/^{16}\text{O}$  ratios. In an ideal world, one standard would be enough, but it is now well established that two-point normalization is a practical requirement for precise isotopic metrology [30, 36]. As a result, an equally important objective is to constrain, as accurately as possible, the relative triple oxygen isotope compositions of carbonate reference materials spanning a wide range of oxygen-18 compositions.

Here, we take advantage of the exceptional metrological properties of a novel spectroscopic technique (VCOF-CRDS: V-shaped Cavity Optical Feedback / Cavity Ring-Down Spectroscopy), to precisely characterize the relative triple-oxygen compositions of  $\text{CO}_2$  equilibrated with three international water reference materials (VSMOW2, SLAP2, GRESP) and  $\text{CO}_2$  produced by phosphoric acid digestion of six international carbonate reference materials (NBS18, NBS19, IAEA603, IAEA610, IAEA611, IAEA612). These observations robustly constrain the relative compositions among the carbonate standards, in a manner fully consistent with the currently accepted relative compositions of VSMOW2 and SLAP2. These relative compositions, particularly those of NBS18 and IAEA603, are critical for normalizing past and future carbonate analyses: adopting an inaccurate ratio  $[^{17}\text{O}/^{16}\text{O}]_{\text{NBS18}}/[^{17}\text{O}/^{16}\text{O}]_{\text{IAEA603}}$  would yield inconsistent scaling factors between measurements normalized to VSMOW-SLAP and those normalized using carbonate standards, potentially introducing large metrological artifacts.

It should be clear that these new observations are only anchored to the VSMOW-SLAP scale inasmuch as we know the triple-oxygen fractionations associated with  $\text{H}_2\text{O}-\text{CO}_2$  equilibration, which are arguably still a matter of debate (e.g. [19] vs [37]). Our results will nevertheless provide robust constraints to be combined with current and future estimates of these fractionation factors.

The findings we report here depend critically on the precision and accuracy of our VCOF-CRDS measurements. The first part of this study is thus dedicated to systematic tests establishing the analytical precision and metrological linearity of our methods. We then report our observations regarding the water and carbonate standards, before discussing how these results may be reconciled with independent observations obtained using very different methods.

## 2 Materials and Methods

### 2.1 Notations

Following the convention widely used in spectroscopic databases such as HITRAN [38], we note  $\text{CO}_2$  isotopologues according to the last digit of each isotope’s mass, so that 626, 627, 628, and 636 stand for  $^{16}\text{O}^{12}\text{C}^{16}\text{O}$ ,  $^{16}\text{O}^{12}\text{C}^{17}\text{O}$ ,  $^{16}\text{O}^{12}\text{C}^{18}\text{O}$  and  $^{16}\text{O}^{13}\text{C}^{16}\text{O}$  respectively. Abundance ratios of rare isotopologues normalized to 626 are noted  $^{627}\text{R}$ ,  $^{628}\text{R}$ ,  $^{636}\text{R}$ . Isotope ratios use a similar notation: “absolute” ratios of a given sample  $x$  are noted  $(^{17}\text{R}^x, ^{18}\text{R}^x, ^{13}\text{R}^x)$ , while ratios relative to VSMOW or VPDB are noted as:

$$\begin{aligned}
^{13}\text{R}_{\text{VPDB}}^x &= ^{13}\text{R}^x / ^{13}\text{R}^{\text{VPDB}} \\
^{17}\text{R}_{\text{VSMOW}}^x &= ^{17}\text{R}^x / ^{17}\text{R}^{\text{VSMOW}} \\
^{18}\text{R}_{\text{VSMOW}}^x &= ^{18}\text{R}^x / ^{18}\text{R}^{\text{VSMOW}}
\end{aligned} \tag{3}$$

Following the usual geochemical convention, stable isotope compositions are noted as small relative deviations from primary reference materials expressed in permil:

$$\begin{aligned}
\delta^{17}\text{O}_{\text{VSMOW}} &= ^{17}\text{R}_{\text{VSMOW}}^x - 1 \\
\delta^{18}\text{O}_{\text{VSMOW}} &= ^{18}\text{R}_{\text{VSMOW}}^x - 1 \\
\delta^{18}\text{O}_{\text{VPDB}} &= ^{18}\text{R}_{\text{VPDB}}^x - 1 \\
\delta^{13}\text{C}_{\text{VPDB}} &= ^{13}\text{R}_{\text{VPDB}}^x - 1
\end{aligned} \tag{4}$$

When making measurements relative to a working reference gas (WG), as we do in this study, we express isotopologue abundances using a similar delta notation:

$$\delta_{628} = ^{628}\text{R}_{\text{WG}}^x - 1 = ^{628}\text{R}^x / ^{628}\text{R}^{\text{WG}} - 1 \tag{5}$$

Here we use the modern logarithmic expression of  $^{17}\text{O}$  anomalies, with a  $\lambda$  value of 0.528 generally considered most relevant for water, carbonate and carbon dioxide compositions [39]:

$$\Delta^{17}\text{O}_{\text{VSMOW}} = \ln(1 + \delta^{17}\text{O}_{\text{VSMOW}}) - \lambda \cdot \ln(1 + \delta^{18}\text{O}_{\text{VSMOW}}) \tag{6}$$

In some situations, such as technical tests and instrumental benchmarks, we consider the *apparent* (non-standardized)  $^{17}\text{O}$  anomaly relative to a working reference gas (WG):

$$\Delta^{17}\text{O}_{\text{WG}} = \ln(1 + \delta_{627}) - \lambda \cdot \ln(1 + \delta_{628}) \tag{7}$$

$\Delta^{17}\text{O}$  values and uncertainties are expressed in permil (‰) or in parts per million (ppm), depending on context.

## 2.2 VCOF-CRDS

V-shaped Cavity Optical Feedback / Cavity Ring-Down Spectroscopy [25, 40, 41] is based on the use of two optical cavities. The VCOF cavity is coupled by optical feedback to a fibered laser diode, resulting in a very stable [42] and ultra-narrow [43] spectral emission. The CRDS cavity is filled with the analyte gas, whose optical absorption is measured using a continuous-wave ring-down approach [44]. Although technical details regarding the optical setup of VCOF-CRDS have been described previously, this is the first time we report VCOF-CRDS measurements on small, static  $\text{CO}_2$  samples (as opposed to continuous flow analyses), using a fibered setup to switch rapidly from one spectral region to another. The technical details of this new approach are provided in Appendix A.

## 2.3 Gas handling within the instrument

Fig. 1 provides a schematic of the gas introduction system. Two identical 1-L tanks, each filled with 3.5 bar of pure  $\text{CO}_2$ , are connected to the inlet system via independent aliquot volumes of 0.6 mL each. Alternatively, gas stored in sealed glass tubes may be introduced using a home-made tube cracker [45]. The gas then expands into the CRDS cavity through a critical orifice whose 30  $\mu\text{m}$  diameter is small

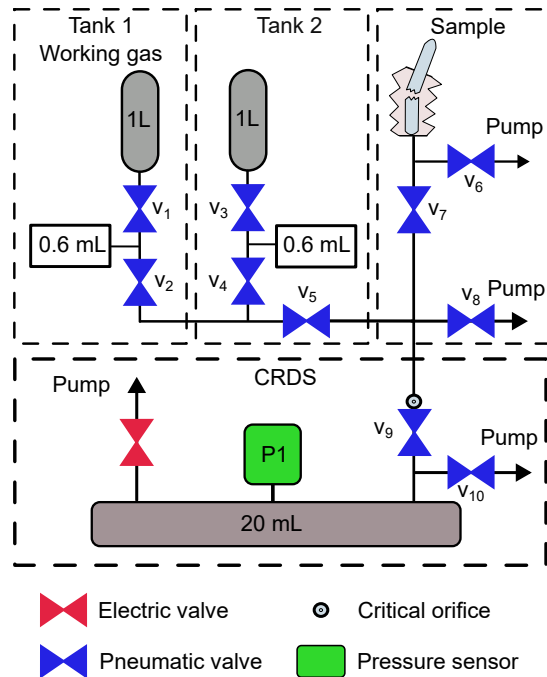


Figure 1 – Schematic of the sample introduction system

enough for a precise control of the final CRDS pressure while maintaining a choked flow regime and minimizing diffusive fractionation ( $0.05 < \text{Knudsen number} < 0.2$ ). The internal volume of the CRDS cell is  $\sim 20$  mL and its pressure are continuously monitored using a Baratron 626D11TBE gauge. Apart from tube cracking, the inlet system is fully automated, allowing the cavity to be filled up to  $5 \pm 0.01$  mbar in a very repeatable manner.

After each analysis, the gas is first slowly evacuated through a proportional solenoid valve until the cell pressure reaches a threshold of 0.1 mbar, then through a larger-diameter valve for at least 180 s. The residual pressure is then less than  $10^{-5}$  mbar.

In practice, this setup allows a single user to perform up to 25–30 analyses per day, manually breaking one ampoule every 20 minutes. A typical daily run comprises 20 analyses of unknown samples and 4 analyses of standards. Measurements performed over a few consecutive days are grouped together into “analytical sessions” for standardization purposes (cf Appendix B). Results are systematically screened for atmospheric contamination (usually due to small leaks), by monitoring two separate absorption lines of the 626 isotopologue. Over the course of this study only two analyses out of  $\sim 200$  were flagged as contaminated.

## 2.4 Water-CO<sub>2</sub> equilibration

We prepare “water-derived” samples by equilibration of CO<sub>2</sub> at 25 °C with various waters of known or unknown triple oxygen compositions (table 1).

A first group of equilibration waters comprises the international reference materials VSMOW2, SLAP2, and GRESP. Although their  $\delta^{18}\text{O}_{\text{VSMOW}}$  values are fixed by convention, the  $\Delta^{17}\text{O}$  values of GRESP and SLAP2 remain for now provisional [35, 46].

A second group of waters comprises three in-house reference materials used at LSCE: HAWAI, OC4, and NEEM, whose compositions are similar to VSMOW2, SLAP2, and GRESP, respectively. The compositions of these standards have been repeatably normalized to VSMOW2 and SLAP2 using IRMS methods.

Group	Water	fraction HAWAI	fraction OC4	fraction NEEM	$\delta^{18}\text{O}_{\text{VSMOW}}$ (‰)	$\Delta^{17}\text{O}_{\text{VSMOW}}$ (‰)	Notes
1	VSMOW2	–	–	–	0	0	
	SLAP2	–	–	–	–55.50	0	$\Delta^{17}\text{O}$ under debate (cf <i>Sharp &amp; Wostbrock, 2021</i> )
	GRESF	–	–	–	–33.40	(0.025)	$\Delta^{17}\text{O}$ provisional ( <i>Vallet-Coulomb et al., 2021</i> )
2	HAWAI	1	–	–	0.54	0.000	known from IRMS measurements at LSCE
	OC4	–	1	–	–53.93	0.009	known from IRMS measurements at LSCE
	NEEM	–	–	1	–32.87	0.038	known from IRMS measurements at LSCE
3	MIX-NH	1/2	–	1/2	–16.17	–0.0171	computed from mix composition
	MIX-OH	1/2	1/2	–	–26.70	–0.0932	computed from mix composition
	MIX-ONH	1/2	1/4	1/4	–21.43	–0.0586	computed from mix composition

Table 1 – Waters used for CO<sub>2</sub> equilibration

Waters of the third and final group are prepared by mixing different proportions of the in-house standards (see table 1): MIX-NH (NEEM + HAWAI), MIX-OH (OC4 + HAWAI) and MIX-ONH (OC4 + NEEM + HAWAI). Based on the end-member compositions and the relative mixing fractions, it is straightforward to predict the triple-oxygen composition of the mixed waters, which have lower  $\Delta^{17}\text{O}$  values than those of the initial waters because of well-understood non-linear mixing effects (fig. 2).

Our water-CO<sub>2</sub> equilibration protocol is adapted from the classical procedure of *Epstein & Mayeda [47]*. We start by degassing a 15-cm-long borosilicate ampoule (4 mm internal diameter), then inject 300  $\mu\text{L}$  water using a long-tipped microsyringe before connecting the ampoule back on the vacuum line. The water is immediately frozen by submerging the lower half of the ampoule in liquid nitrogen. After 5 minutes, the headspace is evacuated down to a baseline pressure of  $10^{-5}$  mbar. At the other end of the vacuum line, we aliquot 40–50  $\mu\text{mol}$  of pure CO<sub>2</sub> from a commercial gas tank (Linde Gas). This CO<sub>2</sub> is first frozen in a liquid nitrogen trap (LNT); potential trace amounts of non-condensable gases are then pumped out. CO<sub>2</sub> is then transferred to a second LNT while the first trap is thawed to  $-80$  °C, ensuring that trace amounts of water and other impurities are not carried over. Finally, CO<sub>2</sub> is transferred to the ampoule (still submerged in liquid nitrogen), which is then flame-sealed, labeled,

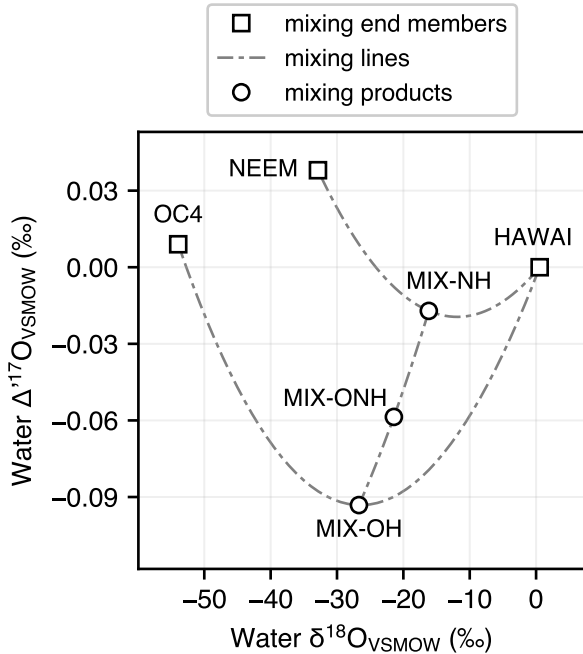


Figure 2 – Triple-oxygen mixing plot showing the water standards analyzed to test the linearity of our  $\Delta^{17}\text{O}$  measurements. The  $\delta^{18}\text{O}$  and  $\Delta^{17}\text{O}$  values of each of the mixing end-members were independently determined by IRMS. Based on well-understood nonlinear mixing effects, the  $\Delta^{17}\text{O}$  values of these six waters are predicted to range from  $-0.09$  to  $+0.4$  ‰.

RM	$\delta^{13}\text{C}_{\text{VPDB}}$ (‰)	$\delta^{18}\text{O}_{\text{VPDB}}$ (‰)	<b>45R</b> CO <sub>2</sub> – 25 °C acid	<b>46R</b> CO <sub>2</sub> – 25 °C acid	$\Delta^{17}\text{O}_{\text{VSMOW}}$ (‰) CO <sub>2</sub> – 90 °C acid	Resulting shift in $\delta^{13}\text{C}_{\text{VPDB}}$ (‰)
NBS18	-5.01	-23.01	0.011900534	0.004089461012	-0.1013	0.007
NBS19	1.95	-2.20	0.011987081	0.004176540992	-0.1304	0.009
IAEA603	2.46	-2.37	0.011992713	0.004175834598	-0.1273	0.009
IAEA610	-9.109	-18.83*	0.011856502	0.004106887765	-0.0691	0.005
IAEA611	-30.795	-4.22*	0.011620151	0.004167790260	-0.0961	0.007
IAEA612	-36.722	-12.08*	0.011550614	0.004134893147	-0.0746	0.005

Table 2 – Nominal isotopic compositions of the carbonates RMs. Values followed by \* are only indicative. Accounting for non-zero  $\Delta^{17}\text{O}$  value would shift  $\delta^{13}\text{C}_{\text{VPDB}}$  values quasi-uniformly by  $7 \pm 2$  ppm.

and stored in a thermally regulated water bath kept at 25 °C for at least three days to achieve complete isotopic equilibrium between water and the CO<sub>2</sub>. During equilibration, only 0.01 % of the water is in vapor phase, so that the isotopic composition of the liquid phase remains the same as that of the water originally injected. About 85 % of the CO<sub>2</sub> is still in the gas phase, with pCO<sub>2</sub> exceeding 500 mbar. The resulting pH of about 4 ensures that over 99 % of the dissolved inorganic carbon is aqueous CO<sub>2</sub>, whose equilibrium oxygen-isotope composition is expected to be very similar to that of gaseous CO<sub>2</sub>, with an experimentally determined offset of  $0.27 \pm 0.16$  ‰,  $1\sigma$  [19, 37, 48].

After three days or longer, each ampoule is taken out of the water bath and its bottom half is immediately submerged in liquid nitrogen. The ampoule is then connected back to the vacuum line through a home-made tube cracker. The liquid nitrogen is then replaced by ethanol kept at –80 °C, thawing the CO<sub>2</sub> while keeping most of the water trapped. The CO<sub>2</sub> is once again trapped in the vacuum line, cryogenically separated from trace water/contaminants, and finally flame-sealed in another, newly degassed borosilicate ampoule, which may be stored indefinitely in the lab.

## 2.5 Acid digestion of carbonates samples

Carbonate samples were processed using an automated sample preparation line, in which ~4 mg of CaCO<sub>3</sub> powder were converted to CO<sub>2</sub> by reaction with 103 % phosphoric acid at 90 °C using a common, stirred acid bath for 15 minutes. After cryogenic removal of water, the resulting CO<sub>2</sub> was transferred to a borosilicate ampoule which was then manually flame-sealed.

We analyzed four IAEA reference materials (IAEA-603, 610, 611, and 612) along with NBS18 and NBS19. Table 2 lists the nominal  $\delta^{13}\text{C}$  and  $\delta^{18}\text{O}$  values for these materials.

## 3 Results

### 3.1 Instrument characterization

#### 3.1.1 Instrumental stability

To assess the instrumental stability of our  $\Delta^{17}\text{O}$  measurements, we analyzed a continuous series of 135 aliquots, alternating between two CO<sub>2</sub> tanks, for a total duration of 27 hours. The uncorrected  $\Delta^{17}\text{O}_{\text{WG}}$  values of each aliquot (defined relative to the long-term average composition of the first tank, treated as the working reference gas) display variations on the order of  $\pm 30$  ppm, but the two tanks covary strongly, so that the short-term offset between them remains quasi-constant (fig. 3). As is commonly done in dual-inlet systems, we may correct for instrumental drifts by defining  $\delta_{636}$ ,  $\delta_{628}$ ,  $\delta_{627}$  values of the second tank relative to the average composition of the two bracketing WG aliquots, yielding “drift-corrected”  $\Delta^{17}\text{O}_{\text{WG}}$

values which are much more repeatable ( $SD = 3.7$  ppm over the whole data set). The scatter in these 67 corrected values appears to behave as random white noise (fig. 4). Drift-corrected  $\delta_{628}$  and  $\delta_{636}$  values are just as stable as  $\Delta^{17}\text{O}_{\text{WG}}$  and almost as repeatable ( $SD = 6\text{-}7$  ppm).

### 3.1.2 Pressure effects

Because the rotovibrational absorption spectrum of a molecular gas depends on its pressure, isotopic measurements by laser spectroscopy often need to be corrected for pressure nonlinearities (e.g., fig. 7 of *Perdue et al.* [28]). In order to check for such effects, we carried out a series of measurements, repeatedly filling the CRDS cavity to different pressures ranging from 4.9 to 5.1 mbar, a pressure range 50 times greater than the operational variability during our CRDS measurements. As shown in fig. 5, the  $\Delta^{17}\text{O}_{\text{WG}}$  values (drift-corrected as described in the previous section) do not appear to vary detectably with analyte pressure, with a standard deviation below 4 ppm, indistinguishable from the previously determined instrumental repeatability of 3.7 ppm (fig. 4).

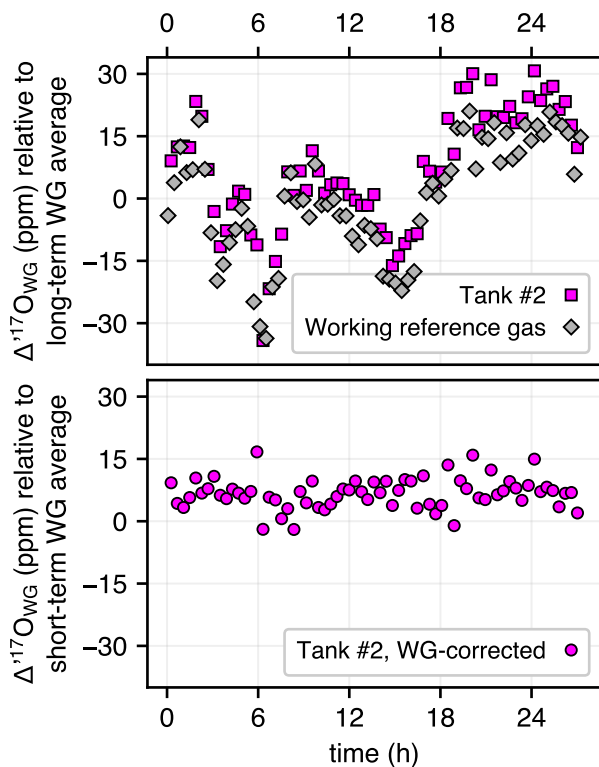


Figure 3 – Instrumental stability over a continuous period of 27 hours. Upper panel: uncorrected  $\Delta^{17}\text{O}$  values of repeated aliquots from two  $\text{CO}_2$  tanks, relative to the overall average composition of one of the tanks (“working reference gas”). Lower panel:  $\Delta^{17}\text{O}$  values of the second tank relative to the preceding and subsequent working-gas measurements.



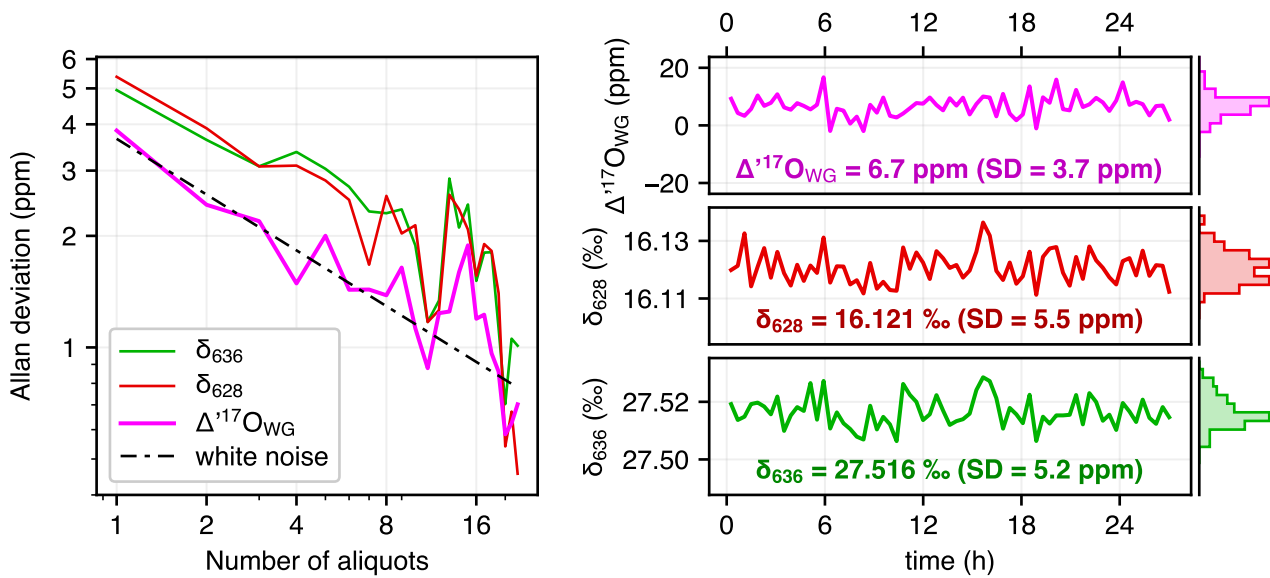


Figure 4 – Allan plot (left) and  $\Delta^{17}\text{O}_{\text{WG}}$ ,  $\delta_{628}$ ,  $\delta_{636}$ , time series corresponding to the working-gas measurements of fig. 3. Analytical scatter of repeated aliquots behaves as expected for white noise.

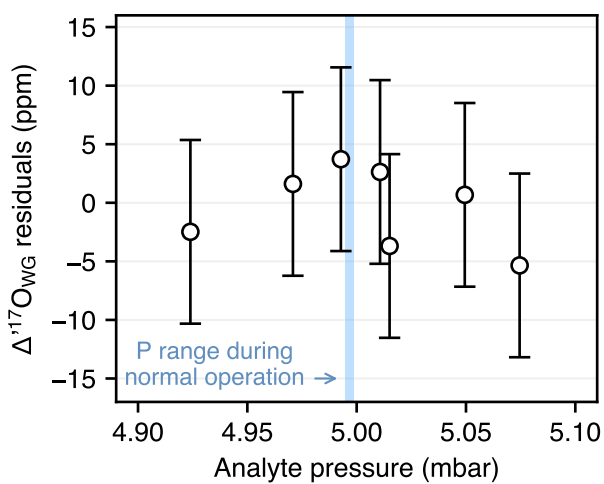


Figure 5 – Absence of pressure effects. Repeated analyses of the same gas, with pressures varying by  $\pm 0.13$  mbar, yield statistically indistinguishable  $\Delta^{17}\text{O}_{\text{WG}}$  values (SD = 3.4 ppm). By comparison, analyte pressure during routine measurements remain within  $\pm 0.002$  mbar.

### 3.1.3 Memory effects

In order to check for memory effects, i.e. whether the results of one analysis are influenced by the composition of the previous analyte, we repeatedly sampled from two CO<sub>2</sub> tanks (A and B) with very different  $\delta^{13}\text{C}$  and  $\delta^{18}\text{O}$  compositions (27 ‰ and 16 ‰ apart, respectively). Two aliquots from each tank were analyzed before switching to the other tank (with WG aliquots interspersed between each analysis, as in section 3.1.1), resulting in the sequence (A-A-B-B-A-A-B-B...). In this experiment, potential memory effects should manifest as detectable differences between the results of consecutive analyses of the same tank, because the first analysis follows one of a very different gas while the second one follows one of a nearly identical analyte. In fig. 6, we compare the measured  $\delta_{636}$  and  $\delta_{628}$  values for the first versus second aliquot of each tank, finding that the two consecutive analyses are always identical within instrumental errors, thus excluding detectable memory effects.

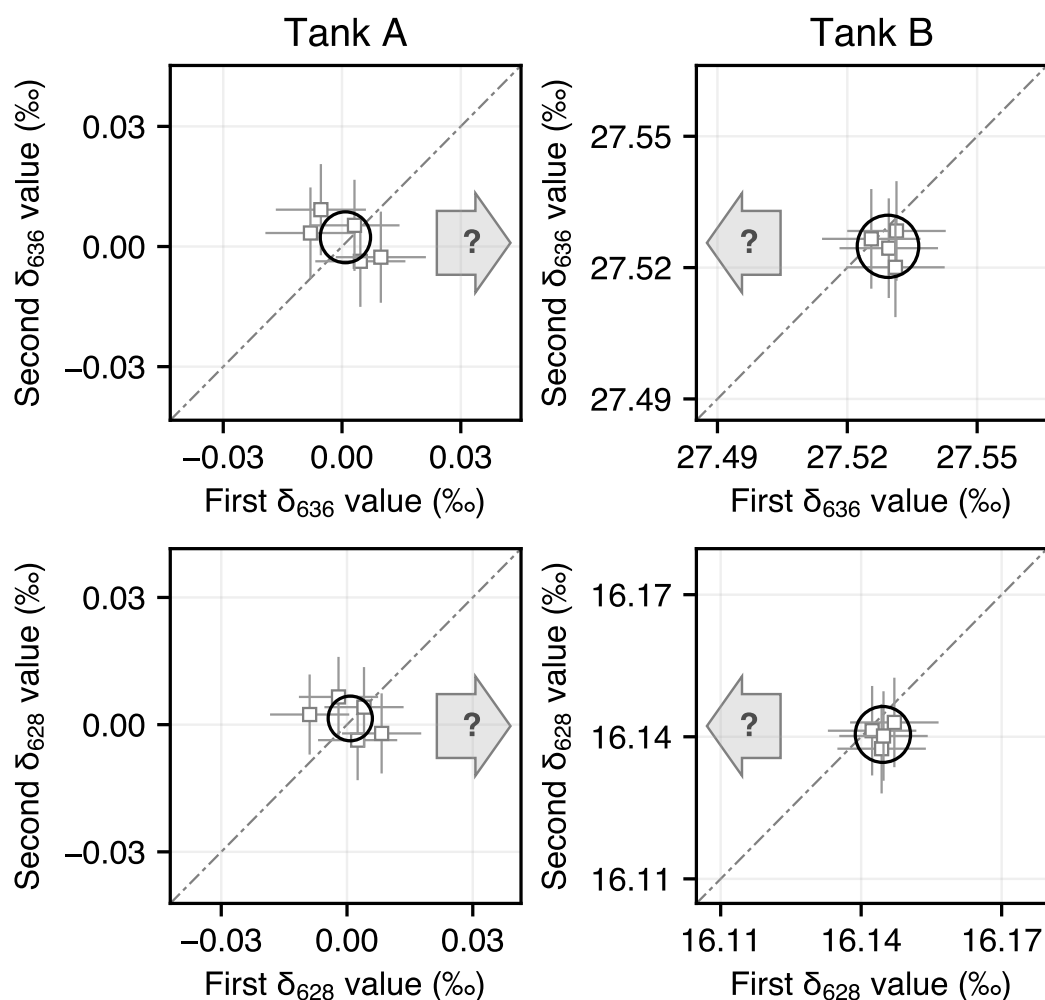


Figure 6 – Absence of memory effects. When aliquots of the same tank are analyzed consecutively, potential memory effects should bias the first analysis in the direction indicated as grey arrows. Individual analyses are shown as squares with 95 % error bars. Black ellipses correspond to joint 95 % confidence limits for the mean of the first and second measured values, based on analytical repeatabilities (SD) of 5.3 ppm and 4.4 ppm for  $\delta_{636}$  and  $\delta_{628}$ , respectively.

## 3.2 Metrological validation

### 3.2.1 $\Delta^{17}\text{O}$ linearity

We test the linearity of our  $\Delta^{17}\text{O}$  measurements by analyzing a suite of  $\text{CO}_2$  samples equilibrated with waters of precisely known triple oxygen compositions with  $\Delta^{17}\text{O}$  values ranging from  $-93$  to  $+38$  ppm (cf section 2.4, table 1, fig. 2).

In these experiments, oxygen isotope ratios in the final state depend only on the equilibrium fractionation parameters  $^{18}\alpha_{\text{CO}_2/\text{H}_2\text{O}}$  and  $\theta_{\text{CO}_2/\text{H}_2\text{O}}$  at  $25^\circ\text{C}$ :

$$\begin{aligned} ^{18}\text{R}^{\text{CO}_2} &= ^{18}\alpha_{\text{CO}_2/\text{H}_2\text{O}} \cdot ^{18}\text{R}^{\text{H}_2\text{O}} \\ ^{17}\text{R}^{\text{CO}_2} &= ^{17}\alpha_{\text{CO}_2/\text{H}_2\text{O}} \cdot ^{17}\text{R}^{\text{H}_2\text{O}} \\ ^{17}\alpha_{\text{CO}_2/\text{H}_2\text{O}} &= \left(^{18}\alpha_{\text{CO}_2/\text{H}_2\text{O}}\right)^{\theta_{\text{CO}_2/\text{H}_2\text{O}}} \end{aligned} \quad (8)$$

However, unless the molar ratio of  $\text{H}_2\text{O}$  to  $\text{CO}_2$  is infinitely large, the final composition of the water will differ slightly from its initial composition. This effect may be computed from the values of  $^{18}\alpha_{\text{CO}_2/\text{H}_2\text{O}}$  and  $\theta_{\text{CO}_2/\text{H}_2\text{O}}$ , imposing conservation constraints on total  $^{16}\text{O}$ ,  $^{17}\text{O}$ ,  $^{18}\text{O}$  and  $\text{CO}_2$  in the system. For any combination of  $^{18}\alpha_{\text{CO}_2/\text{H}_2\text{O}}$  and  $\theta_{\text{CO}_2/\text{H}_2\text{O}}$  values, we may thus predict the  $\Delta^{17}\text{O}$  value of equilibrated  $\text{CO}_2$  as a function of initial  $\text{CO}_2$  composition, initial water composition, and  $\text{H}_2\text{O}/\text{CO}_2$  ratio. As shown in fig. 7, accounting for finite  $\text{H}_2\text{O}/\text{CO}_2$  ratios may result in positive or negative  $\Delta^{17}\text{O}$  offsets relative to the infinite ratio limit, depending on the initial  $\delta^{18}\text{O}$  offset between water and  $\text{CO}_2$ .

Here we use the theoretical  $^{18}\alpha_{\text{CO}_2/\text{H}_2\text{O}}$  and  $\theta_{\text{CO}_2/\text{H}_2\text{O}}$  predictions of *Guo & Zhou* [37] (Suppl. Table 1). Using a different pair of fractionation parameters would shift all water-equilibrated  $\Delta^{17}\text{O}$  values by a constant offset, with no bearing whatsoever on the outcome of our linearity tests. Doing so would, however, similarly offset our  $\Delta^{17}\text{O}$  measurements of carbonate-derived  $\text{CO}_2$  relative to VSMOW, with implications further discussed in section 4.2.

For each water listed in table 1, we performed 4–6 equilibration experiments, with each experiment yielding enough equilibrated  $\text{CO}_2$  for a single analysis. The results were standardized using HAWAI and OC4 as anchors, based on the equilibrated compositions predicted in fig. 7. The overall  $\Delta^{17}\text{O}$  repeatability of these analyses ( $\text{SD} = 4.2$  ppm) is once again indistinguishable from instrumental precision. As shown in fig. 8, the standardized  $\Delta^{17}\text{O}_{\text{VSMOW}}$  values of all equilibrated samples agree almost perfectly with expectations, with residuals ranging from  $-2$  to  $+1$  ppm ( $\text{RMSE} = 1.2$  ppm). Because their respective compositions are predicted almost exclusively from mathematical laws, the three mixed-water samples

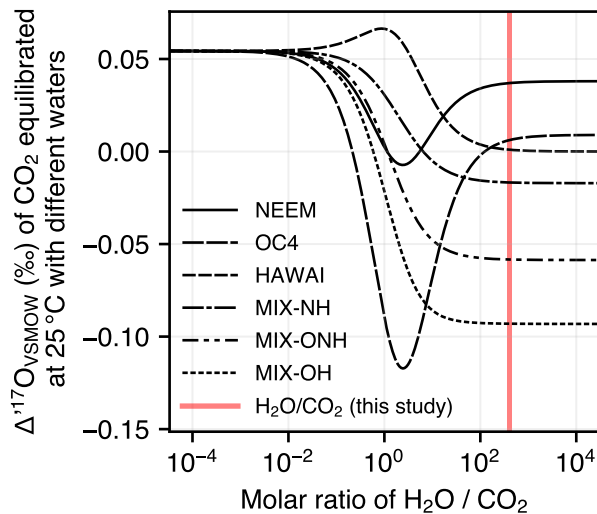


Figure 7 – Predicted  $\Delta^{17}\text{O}$  of water-equilibrated  $\text{CO}_2$  as a function of the molecular ratio  $\text{H}_2\text{O}/\text{CO}_2$ . Due to non-linear mixing effects, final  $\Delta^{17}\text{O}$  of equilibrated  $\text{CO}_2$  depends on  $\text{H}_2\text{O}/\text{CO}_2$  ratio, initial water  $\Delta^{17}\text{O}$ , and relative  $\delta^{18}\text{O}$  values of  $\text{CO}_2$  and  $\text{H}_2\text{O}$ . Initial  $\Delta^{17}\text{O}$  of the  $\text{CO}_2$  tank used in this study is  $-0.084$  ‰. Solid and dashed black lines correspond to the different waters used in this study. The mixing ratio used in our experiments ( $\sim 400$ ) is shown as a vertical red line.

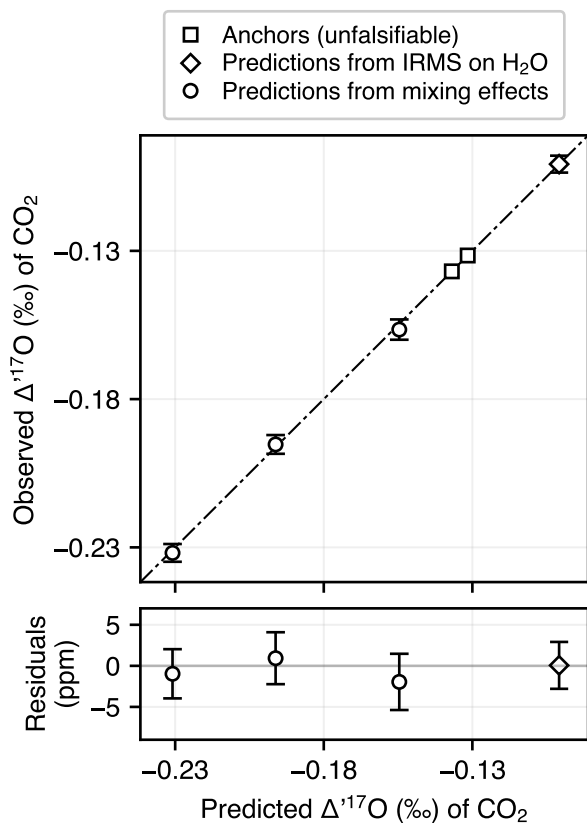


Figure 8 – Quasi-perfect agreement between the predicted and measured  $\Delta^{17}\text{O}_{\text{VSMOW}}$  values of  $\text{CO}_2$  equilibrated with waters of independently known compositions. One may reasonably expect that the range of  $\Delta^{17}\text{O}_{\text{VSMOW}}$  values sampled here is larger than the natural variability of most carbonates.

testify to the linearity of our measurements. Additionally, the “perfect” agreement (0.0 ppm) between our result for NEEM and the results of independent IRMS measurements demonstrate that  $\Delta^{17}\text{O}$  values derived from the two techniques are directly comparable.

### 3.2.2 $\delta^{13}\text{C}$ linearity

All of the  $\text{CO}_2/\text{H}_2\text{O}$  equilibration experiments reported in the previous section were performed using the same initial  $\text{CO}_2$ . However, the carbonate reference materials that we aim to characterize have variable  $\delta^{13}\text{C}$  values. In order to rule out “cross-talk” between the absorption lines that we are targeting, i.e. to test whether our final, standardized  $\Delta^{17}\text{O}_{\text{VSMOW}}$  values may depend on the carbon-13 composition of analytes, we performed another experiment where we equilibrated VSMOW2 and SLAP2 with  $\text{CO}_2$  from two tanks with  $\delta^{13}\text{C}$  values about 25 ‰ apart (i.e. over three times the  $\delta^{13}\text{C}$  offset between NBS18 and IAEA603). In this experiment, we treat the  $^{13}\text{C}$ -rich samples as standardization anchors, so that the corresponding water  $\Delta^{17}\text{O}_{\text{VSMOW}}$  values are zero by definition, while the  $^{13}\text{C}$ -depleted samples are treated as unknowns, yielding apparent water  $\Delta^{17}\text{O}_{\text{VSMOW}}$  values of  $+0.9 \pm 7.0$  ppm and  $-0.7 \pm 6.7$  ppm, ruling out any instrumentally significant bias associated with  $\delta^{13}\text{C}$ .

## 3.3 Characterization of international carbonate reference materials

### 3.3.1 Analytical repeatability of phosphoric acid reactions

We tested whether the conversion of carbonates to  $\text{CO}_2$  by phosphoric acid reaction introduces additional analytical noise by comparing the  $\Delta^{17}\text{O}_{\text{WG}}$  values of 8  $\text{CO}_2$  samples independently produced from the same Carrara marble standard. The standard deviation of these 8 data points is 4.3 ppm, statistically indistinguishable from the instrumental repeatability determined in section 3.1.1. Based on our accumulated laboratory experience since that experiment, we find that the operational repeatability of  $\Delta^{17}\text{O}$

measurements on carbonates of variable compositions, at the scale of weeks or months, is slightly larger, on the order of 6 ppm, potentially due to acid bath memory effects, different acid concentrations and/or sample degassing conditions.

### 3.3.2 Reference material results

In a first series of measurements, we analyzed together all the international reference materials (RMs) listed in tables 1-2, comprising three water RMs (VSMOW2, SLAP2, GRESP) and six carbonate RMs used for  $\delta^{18}\text{O}$  and/or  $\delta^{13}\text{C}$  standardization to the VPDB scale (NBS18/19, IAEA603, IAEA610/611/612). In a second series of measurements spanning another six months, we repeatedly reanalyzed VSMOW2, SLAP2, IAEA603 and NBS18, to better constrain the relative compositions of the two carbonate RMs, which will likely be a critical piece of information used to standardize analytical results across laboratories. For all of the above data,  $\text{CO}_2$  equilibrated with VSMOW2 and SLAP2 were treated as standardization anchors, with nominal  $\delta^{18}\text{O}$  and  $\Delta^{17}\text{O}$  values computed, as above, based on the theoretical  $^{18}\alpha_{\text{CO}_2/\text{H}_2\text{O}}$  and  $\theta_{\text{CO}_2/\text{H}_2\text{O}}$  values of *Guo & Zhou* [37]. The carbonate measurements were also independently standardized to the VPDB scale, using (NBS18/19 and IAEA603) as anchors for  $\delta^{18}\text{O}_{\text{VPDB}}$  and (NBS19, IAEA603/610/611/612) as anchors for  $\delta^{13}\text{C}_{\text{VPDB}}$ , as recommended by *Hillaire-Marcel et al.* [36] and *Assonov et al.* [49]. All results are summarized in table 3 and fig. 9.

The oxygen-18 water composition computed from our GRESP-equilibrated measurements is  $\delta^{18}\text{O}_{\text{VSMOW}} = -33.42 \pm 0.03 \text{ ‰}$  (1SE), consistent with GRESP's reference value of  $-33.40 \pm 0.04 \text{ ‰}$  (1SE). Its  $\Delta^{17}\text{O}_{\text{VSMOW}}$  value is  $0.035 \pm 0.007 \text{ ‰}$  (95% CL), within analytical uncertainties of a previous, independent measurement (*Vallet-Coulomb et al.* [46]:  $0.025 \pm 0.010 \text{ ‰}$ , 2SE).

In light of the standardization issues discussed in the next section, we specifically checked the stability, over a period of nine months, of our results for IAEA603 and NBS18. Measurements of the two standards display no obvious drift over time, and as shown in fig. 10, the offset between their  $\Delta^{17}\text{O}$  values is virtually identical in early 2023, when only reference materials were analyzed, as in late 2023, when IAEA603, NBS18, VSMOW2 and SLAP2 were routinely analyzed along with natural water and carbonate samples of various origins (not discussed here).

Sample	Type	N	Predicted	$\delta^{18}\text{O}_{\text{VSMOW}}$			$\Delta^{17}\text{O}_{\text{VSMOW}}$			$\delta^{13}\text{C}_{\text{VPDB}}$			$\delta^{18}\text{O}_{\text{VPDB}}$		
			$\Delta^{17}\text{O}_{\text{VSMOW}}$	(‰)	SD	$\pm$ (95%)	(‰)	SD	$\pm$ (95%)	(‰)	SD	$\pm$ (95%)	(‰)	SD	$\pm$ (95%)
VSMOW2-CO2	W	23	-0.1365	41.34*	0.04	-	-0.1365*	0.0080	-	-	-	-	-	-	-
SLAP2-CO2	W	24	-0.1417	-16.07*	0.05	-	-0.1417*	0.0050	-	-	-	-	-	-	-
HAWAI-CO2	W	5	-0.1369	41.94*	0.07	-	-0.1369*	0.0046	-	-	-	-	-	-	-
OC4-CO2	W	6	-0.1316	-14.51*	0.04	-	-0.1316*	0.0052	-	-	-	-	-	-	-
NEEM-CO2	W	6	-0.1008	7.17	0.30	0.22	-0.1008	0.0033	0.0030	-	-	-	-	-	-
MIX-NH-CO2	W	4	-0.1546	24.55	0.28	0.26	-0.1566	0.0029	0.0036	-	-	-	-	-	-
MIX-ONH-CO2	W	5	-0.1962	19.27	0.26	0.24	-0.1953	0.0034	0.0034	-	-	-	-	-	-
MIX-OH-CO2	W	6	-0.2309	13.77	0.26	0.22	-0.2319	0.0035	0.0032	-	-	-	-	-	-
GRESP-CO2	W	6	-	6.75	0.03	0.06	-0.1037	0.0120	0.0066	-	-	-	-	-	-
NBS18-CO2	C	23	-	15.57	0.19	0.03	-0.1013	0.0108	0.0033	-5.03	0.09	0.07	-23.01*	0.16	-
NBS19-CO2	C	4	-	37.20	0.01	0.07	-0.1304	0.0033	0.0076	1.95*	0.04	-	-2.2*	0.00	-
IAEA603-CO2	C	26	-	36.83	0.09	0.03	-0.1273	0.0068	0.0036	2.46*	0.03	-	-2.37*	0.09	-
IAEA610-CO2	C	6	-	19.93	0.06	0.05	-0.0691	0.0062	0.0060	-9.109*	0.11	-	-18.82	0.07	0.11
IAEA611-CO2	C	6	-	34.93	0.10	0.05	-0.0961	0.0049	0.0064	-30.795*	0.05	-	-4.28	0.10	0.11
IAEA612-CO2	C	6	-	26.88	0.05	0.05	-0.0746	0.0065	0.0061	-36.722*	0.02	-	-12.08	0.05	0.10

Table 3 – Compiled analytical results. Values followed by \* were used as anchors for isotopic standardisation, and thus do not have quote confidence limits.

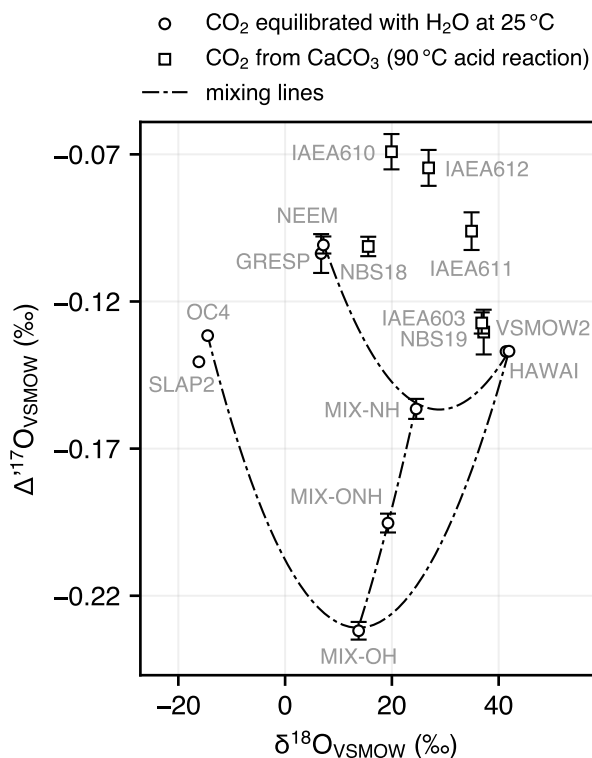


Figure 9 – Triple oxygen isotope compositions of samples analyzed in this study. Error bars are 95 % confidence limits. Samples without error bars are standardization anchors whose compositions are postulated a priori. Note that equilibrating water RMs with CO<sub>2</sub> and reacting carbonate RMs yields CO<sub>2</sub> samples with δ<sup>18</sup>O values in the same range. As a result, our carbonate-derived samples are directly comparable to CO<sub>2</sub> equilibrated with VSMOW2 or with our mixed water samples, regardless of potential compositional nonlinearities.

## 4 Discussion

### 4.1 Updated realization of the VPDB scale for δ<sup>13</sup>C

As part of ongoing international efforts to improve the accuracy and reproducibility of δ<sup>13</sup>C measurements on CO<sub>2</sub>, with a stated goal of ±0.01 ‰ accuracy [50], three new carbonate reference materials were recently introduced (IAEA610, IAEA611, IAEA612), which are intended to allow δ<sup>13</sup>C standardization to the VPDB scale based on two or more standards, in a similar way to VSMOW-SLAP standardization [49].

With the rapidly increasing use of spectroscopic methods, it is worthwhile to assess the Δ<sup>17</sup>O values of the reference materials underpinning the δ<sup>13</sup>C<sub>VPDB</sub> scale. The δ<sup>13</sup>C value coming out of IRMS is computed by correcting the 45/44 and 46/44 ion beam ratios assuming Δ<sup>17</sup>O = 0 [51], while that obtained from infra-red absorption spectroscopy directly probes the abundance ratio 636/626. These are actually two different mathematical quantities (neither of which is strictly equivalent to the canonical definition of δ<sup>13</sup>C, which nominally includes multiply-substituted isotopologues subject to clumped-isotope anomalies, such as 638). If the four RMs IAEA603/610/611/612 all have non-zero yet very similar Δ<sup>17</sup>O values, δ<sup>13</sup>C measurements standardized using them will not depend on which technique was used. Otherwise, the VPDB scale realization will not remain consistent across the IRMS/spectroscopy divide.

The Δ<sup>17</sup>O<sub>VSMOW</sub> values we obtain for the six carbonate standards (after acid conversion to CO<sub>2</sub>) range from −0.13 to −0.07 ‰ and are listed in table 2. These non-zero values, if accounted for when correcting 45/44 ion ratios, imply that the true 636/626 ratios of the RMs are 5–9 ppm greater than predicted from their nominal δ<sup>13</sup>C values. Although the average 7 ppm shift may conceivably become metrologically significant at some point in the future, for now the very small spread of offsets implies that the realization of the δ<sup>13</sup>C VPDB scale using these RMs will remain consistent whether using laser or IRMS measurements. If/when additional VPDB RMs are introduced in the future, however, we recommend characterizing and reporting their oxygen-17 compositions as was done here.

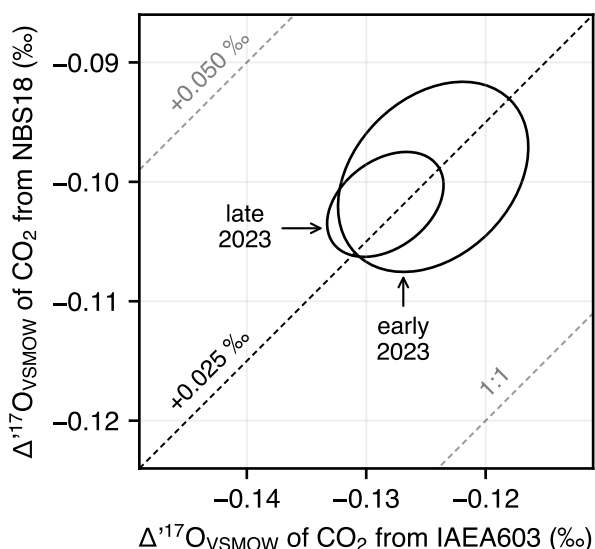


Figure 10 – Comparison of  $\Delta^{17}\text{O}$  values obtained for IAEA603 and NBS18 over different measurements periods. In early 2023, only the reference materials discussed in this study were analyzed, whereas data of late 2023 are RM measurements used to routinely standardize natural water and carbonate samples of various origins.

## 4.2 Inter-laboratory comparison of carbonate $\Delta^{17}\text{O}$ measurements

### 4.2.1 $\Delta^{17}\text{O}$ offsets and common patterns

The precise oxygen-17 composition of the international carbonate reference materials underpinning the oxygen-18 VPDB scale has been under active investigation for at least a decade using different techniques including quantitative conversion of  $\text{CO}_2$  to  $\text{O}_2$  by various methods [3, 12, 14, 33] and platinum-catalyzed steady-state exchange between  $\text{O}_2$  and  $\text{CO}_2$  [32, 34, 52]. The spread of  $\Delta^{17}\text{O}_{\text{VSMOW}}$  values obtained by different groups for NBS18, NBS19 and IAEA603 is summarized in fig. 11.

It is immediately apparent that the values reported for any given standard (only including acid-reaction  $\text{CO}_2$  products) vary by up to 80–140 ppm, which is an order of magnitude greater than the analytical uncertainties reported in the original publications. As pointed out in some of these studies, the most plausible reasons for these inter-laboratory discrepancies are incomplete conversion of  $\text{CO}_2$  to  $\text{O}_2$  and/or various types of uncorrected instrumental “nonlinearities”, a nonspecific term referring to various kinds of systematic analytical errors.

Nevertheless, the  $\Delta^{17}\text{O}$  values of the two marble standards (IAEA603 and NBS19) reported by any given laboratory tend to be very similar, with NBS18 values always greater than for the marbles, by several tens of ppm. As seen in Figures 10-11, our own results follow the same pattern, with statistically indistinguishable  $\Delta^{17}\text{O}$  for NBS19 and IAEA603, and an NBS18 value greater than that of IAEA603 by  $26 \pm 5$  ppm (95 % CL).

### 4.2.2 Potential causes for $\Delta^{17}\text{O}$ discrepancies

First, it bears repeating that our measurements are ultimately tied to the VSMOW-SLAP scale by  $\text{CO}_2$  equilibrated at 25 °C with various water RMs, assuming an oxygen-18 fractionation factor  $^{18}\alpha_{\text{CO}_2/\text{H}_2\text{O}}$  of 1.041461 and a  $\theta_{\text{CO}_2/\text{H}_2\text{O}}$  exponent of 0.5246 after *Guo & Zhou* [37]. Using numerically different fractionation parameters would potentially shift all of our final  $\Delta^{17}\text{O}_{\text{VSMOW}}$  values, uniformly, by tens of ppm. For instance, had we chosen to use the fractionation parameters determined experimentally at the Hebrew University of Jerusalem (HUJ) by *Barkan & Luz* [19],  $^{18}\alpha_{\text{CO}_2/\text{H}_2\text{O}} = 1.041036$  and  $\theta_{\text{CO}_2/\text{H}_2\text{O}} = 0.5229$ , our results for the six carbonate RMs would have been indistinguishable (within analytical uncertainties) from those obtained by the HUJ group (fig. 12). Although opting for the *Guo & Zhou* [37] parameters puts our final  $\Delta^{17}\text{O}_{\text{VSMOW}}$  values much closer to the median  $\text{CO}_2$  values obtained by other groups, for

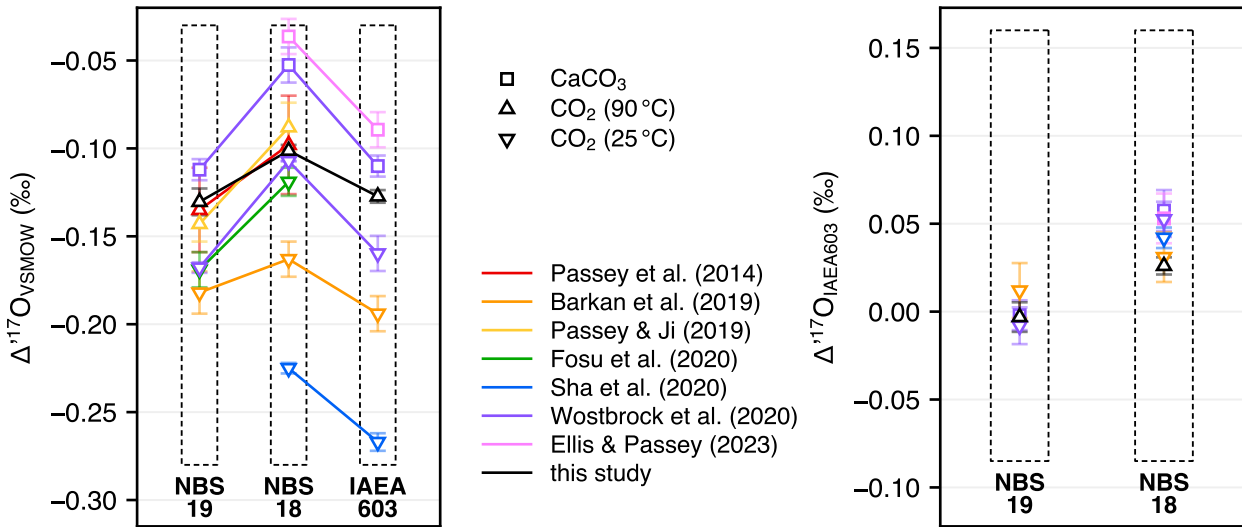


Figure 11 – Comparison with previously reported  $\Delta^{17}\text{O}$  values. The data shown here were slightly corrected, for consistency, to use the same nominal value  $\Delta^{17}\text{O}_{\text{VSMOW}}^{\text{SLAP}}$ . Results reported by *Hare et al.* [27] and *Perdue et al.* [28] are not shown here because their measurements were standardized using values reported by *Wostbrock et al.* [12]. In the right-hand panel, plotting  $\Delta^{17}\text{O}$  values relative to IAEA603 (by simple subtraction, with propagated uncertainties), highlights the spread of  $\Delta^{17}\text{O}_{\text{IAEA603}}^{\text{NBS18}}$  values obtained by different groups.

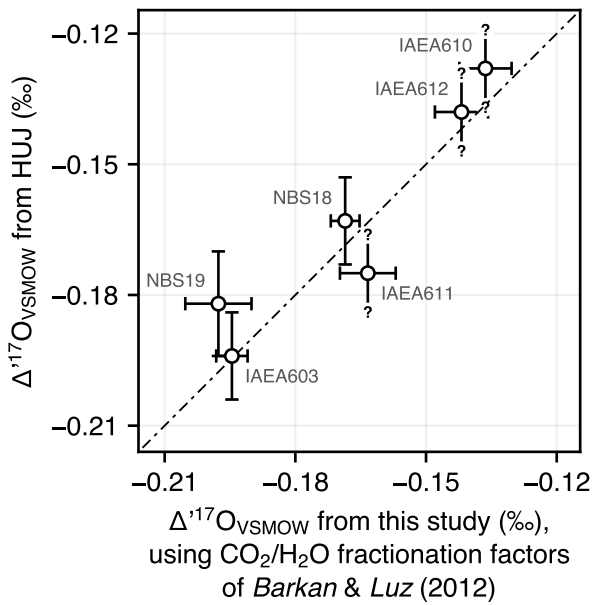


Figure 12 – Comparison between our results and those from the Hebrew University of Jerusalem (HUJ), assuming  $^{18}\alpha_{\text{CO}_2/\text{H}_2\text{O}} = 1.041036$  and  $\theta_{\text{CO}_2/\text{H}_2\text{O}} = 0.5229$  after *Barkan & Luz* [19]. HUJ data from *Barkan et al.* [53] and *Assonov* [54].



now this choice remains mostly arbitrary, and we acknowledge that our results only truly constrain the following sum of three quantities:

$$\Delta^{17}\text{O}_{\text{VSMOW}} + (\theta_{\text{CO}_2/\text{CaCO}_3} - \lambda) \cdot \ln(^{18}\alpha_{\text{CO}_2/\text{CaCO}_3}) - (\theta_{\text{CO}_2/\text{H}_2\text{O}} - \lambda) \cdot \ln(^{18}\alpha_{\text{CO}_2/\text{H}_2\text{O}}) \quad (9)$$

with  $\text{CO}_2/\text{CaCO}_3$  and  $\text{CO}_2/\text{H}_2\text{O}$  denoting fractionations from phosphoric acid reaction at 90 °C and water- $\text{CO}_2$  equilibration at 25 °C, respectively. Reprocessing our data based on different fractionation parameters should be straightforward using our public source code repository (<https://doi.org/10.5281/zenodo.14007201>).

Secondly, the observations reported here cannot be used to discriminate between different proposed values for the true oxygen-17 composition of SLAP2, e.g.,  $\Delta^{17}\text{O}_{\text{VSMOW}}^{\text{SLAP2}} = 0$  as conventionally assumed versus  $\Delta^{17}\text{O}_{\text{VSMOW}}^{\text{SLAP2}} = -15$  ppm as proposed by *Wostbrock et al.* [12], or  $\Delta^{17}\text{O}_{\text{VSMOW}}^{\text{SLAP2}} = -11$  ppm as proposed by *Sharp & Wostbrock* [35]. Reprocessing our data using any of these assumptions would yield self-consistent results, with changes to all of our final  $\Delta^{17}\text{O}_{\text{VSMOW}}$  values being exactly equal to:

$$\ln(1 + \delta^{18}\text{O}_{\text{VSMOW}}) / \ln(1 - 0.0555) \cdot \Delta^{17}\text{O}_{\text{VSMOW}}^{\text{SLAP2}} \quad (10)$$

In particular, all our tests of linearity would yield identical answers, including the mixed-waters experiment of fig. 8. From this point onward, as was done in 11, when comparing observations between groups we systematically recompute the originally reported values, using the above formula, to be consistent with  $\Delta^{17}\text{O}_{\text{VSMOW}}^{\text{SLAP2}} = 0$ , eliminating one (minor) source of discrepancy.

Thirdly, the  $\Delta^{17}\text{O}$  difference between NBS18 and IAEA603 determined here ( $26 \pm 5$  ppm, hereafter noted  $\Delta^{17}\text{O}_{\text{IAEA603}}^{\text{NBS18}}$ ) is statistically indistinguishable from that of *Barkan et al.* [53] ( $31 \pm 14$  ppm), but substantially smaller than that reported by other groups, ranging from  $42 \pm 6$  ppm to  $68 \pm 21$  ppm. The fact that independent groups using different techniques would obtain similar results is not particularly telling in itself, since it applies both to the low end (*Barkan et al.* and this study) and the high end (*Wostbrock et al.* [12] and *Ellis & Passey* [14]) of the values proposed for  $\Delta^{17}\text{O}_{\text{IAEA603}}^{\text{NBS18}}$ . The fact that our estimate of  $\Delta^{17}\text{O}_{\text{IAEA603}}^{\text{NBS18}}$  is the smallest reported to date necessarily inspires caution, however. Below, we discuss potential sources of error in our measurements and how they may affect our finding.

In their review of these issues, *Sharp & Wostbrock* [35] remarked that “the difference in the  $\Delta^{17}\text{O}$  values between any two standards should be the same for all laboratories”. This statement makes two implicit assumptions: (a) that the calcite standards were fractionated uniformly by the chemical reactions used within each laboratory; (b) that the net effect of instrumental nonlinearities, after performing all analytical corrections, is a constant, lab-specific offset of  $\Delta^{17}\text{O}$ .

Assumption (a) often goes unchallenged. For example,  $\text{CO}_2/\text{H}_2\text{O}$  equilibration and phosphoric acid reactions are known to fractionate oxygen isotopes in a repeatable manner within a few tens of ppm. Each method has its own caveats, however. For example, acid digestion of some natural samples may release trace amounts of contaminants which may interfere with IRMS and/or spectroscopic measurements (e.g., *Fiebig et al.* [55]). Fluorination of carbonates may convert various oxygen-bearing phases other than calcite (e.g., fluid inclusions, carbonate associated sulfate, dolomite, apatite) into  $\text{O}_2$ , many of which would not be converted to  $\text{CO}_2$  by acid digestion. In light of this, one notable difference between NBS18 carbonatite and NBS19/IAEA603 marble is that the former is less chemically pure, with potentially several % (poorly constrained) Fe-dolomite and trace amounts (<1 %) of quartz and apatite [56]. Additionally, Pt-catalyzed  $\text{CO}_2\text{-O}_2$  exchange may be biased by variable thermal-gradient-induced fractionations [57]. Such biases, however, may remain constant when analyzing NBS18 and IAEA603 under the same experimental conditions. At this stage it would seem difficult to claim that any one of these chemical pathways is inherently superior to the others.

Even if we accept that all of these methods consistently preserve/fractionate oxygen isotopes during chemical conversions, we should still be mindful that assumption (b) above may not be strictly true. In other words, we should consider the possibility that even after applying two-point standardization, residual instrumental artefacts could manifest as  $\Delta^{17}\text{O}$  scale compression/expansion, and/or  $\delta^{18}\text{O}$ - or  $\delta^{13}\text{C}$ -dependent biases. Such nonlinearities are for example well documented for clumped-isotope measurements of  $\Delta_{47}$  in  $\text{CO}_2$  [58–60]. Although the process believed to cause  $\Delta_{47}$  scale compression in Nier-type ion sources is unlikely to affect  $\Delta^{17}\text{O}$ , compositional and/or pressure-dependent nonlinearities caused by inaccurate estimates of background levels (“pressure baseline effects”) are directly relevant to  $\Delta^{17}\text{O}$  measurements [61]. To the first order, such background errors will bias measured  $\Delta^{17}\text{O}$  values in a way that is proportional to  $\delta^{17}\text{O}$ , so that a simple two-point correction approach (e.g., using VSMOW2 and SLAP2, as we did here) may be sufficient to correct them. But to the second order, “pressure baseline effects” may have a quadratic component which will not be corrected by two-point standardization, depending on how exactly the true background levels vary with the primary ion beam, and/or on the exact data processing used for corrections (cf fig. 7 of *He et al.* [59]).

As a thought experiment, one may ask how strong a quadratic correction to our data would be needed to make our results exactly consistent with the  $\Delta^{17}\text{O}_{\text{IAEA603}}^{\text{NBS18}}$  estimate published by *Wostbrock et al.* [12], which has been used to normalize the measurements of subsequent studies [27, 28]. This hypothetical quadratic nonlinearity is shown in fig. 13A. Following this hypothesis, the results of our mixed water experiments would have to be systematically biased by up to 38 ppm, which is highly unlikely based on the excellent agreement between our predictions and observations (fig. 8). Conversely, one may attempt to quantify the quadratic correction needed to perfectly reconcile the  $\Delta^{17}\text{O}_{\text{IAEA603}}^{\text{NBS18}}$  value reported by *Wostbrock et al.* [12] with our own findings. In that case, a much smaller quadratic correction would be sufficient, corresponding to systematic errors in the VSMOW2-SLAP2 range not exceeding 8-9 ppm (fig. 13B). With an even smaller quadratic correction remaining below 5 ppm over the whole VSMOW2-SLAP2 range, the *Wostbrock et al.* [12]  $\text{CO}_2$  values for IAEA603 and NBS18 (reacted at 25 °C) would become indistinguishable from our own within analytical uncertainties. Although perhaps counter-intuitive, the striking difference between these two simulations is a direct consequence of the different distributions of  $\delta^{18}\text{O}$  values between unknowns (IAEA603 and NBS18) and anchors (VSMOW2 and SLAP2) in the two studies.

It should be very clear that this thought experiment is not intended to establish whether any particular data set is flawed. Instead, it should highlight how much the relative oxygen-18 compositions of anchor and unknown analytes can either dampen or amplify the magnitude of instrumental nonlinearities without introducing additional hypotheses. Based on the simple simulation of fig. 13, it appears that such hypothetical quadratic nonlinearities, while small enough to remain unnoticed in routine measurements, should be detectable in carefully designed experiments such as our mixed water tests.

#### 4.2.3 Provisional recommendations

At this point, we put forward that the results reported here demonstrate the outstanding precision and linearity of our VCOF-CRDS measurements, and we stand by the relative  $\Delta^{17}\text{O}$  values reported here for carbonate reference materials. However, because these values are inherently tied to an arbitrary choice of ( $^{18}\alpha_{\text{CO}_2/\text{H}_2\text{O}}$ ,  $\theta_{\text{CO}_2/\text{H}_2\text{O}}$ ), and in view of lingering inter-laboratory discrepancies, we advocate that, for now, the oxygen-17 composition of carbonates should systematically be reported relative to IAEA603 in addition to VSMOW (for example using the explicit notation  $\Delta^{17}\text{O}_{\text{IAEA603}}$ ), using two-point normalization based on one more carbonate standard such as NBS18. This suggestion closely mirrors the use of a VPDB scale to report carbonate  $\delta^{18}\text{O}$  measurements while still preserving the primary status of VSMOW.

Using two-point standardization will still require some conventional choice regarding the nominal oxygen-17 composition of NBS18. For now, reporting of carbonate  $\Delta^{17}\text{O}_{\text{IAEA603}}$  values should thus

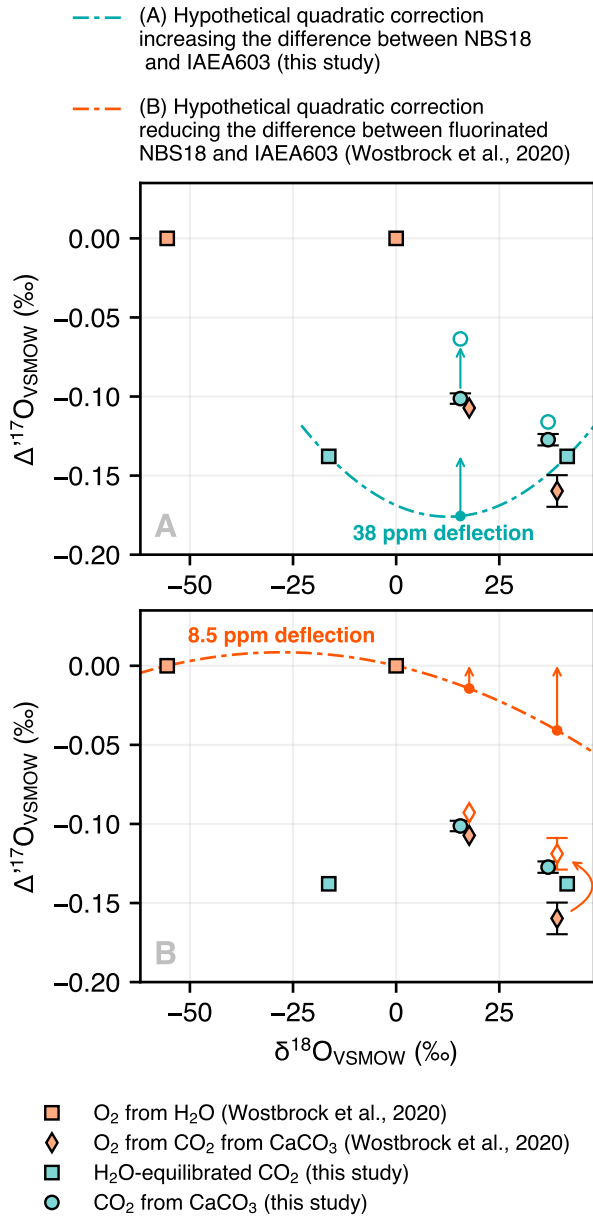


Figure 13 – Thought experiment testing whether our results and those of Wostbrock et al. [12] may be reconciled by correcting for (purely hypothetical) quadratic nonlinearities. Error bars are 95 % confidence limits. (A) Reconciling our  $\Delta^{17}\text{O}_{\text{IAEA603}}^{\text{NBS18}}$  estimate to agree with Wostbrock et al. [12] by postulating a quadratic instrumental artefact would imply systematic errors of up to 38 ppm, at odds with the excellent metrological linearity shown in fig. 8 (B) By contrast, a much smaller quadratic artifact would be enough to make the  $\Delta^{17}\text{O}_{\text{IAEA603}}^{\text{NBS18}}$  estimate of Wostbrock et al. [12] consistent with ours. This large difference is due to different distributions of  $\delta^{18}\text{O}$  values for the carbonate-derived analytes relative to the water-derived ones.

always specify the exact  $\Delta^{17}\text{O}$  difference postulated between NBS18 and IAEA603. Doing so should greatly facilitate reprocessing these results once we have better constraints on the true relationship between carbonate and water reference materials.

## 5 Conclusion

Considerable efforts and ingenuity have been expended over the years to transfer the triple oxygen isotope composition of  $\text{CaCO}_3$  or  $\text{CO}_2$  to other molecules, bypassing isobaric interference issues. Over the same period, independent efforts to improve the metrological performance of infra-red absorption spectroscopy have also achieved remarkable progress. Today, we are probably within reach of a consensus regarding the quantitative relationships between triple oxygen isotopes in water, molecular oxygen, carbonates, and other minerals such as silicates (e.g., *Sharp & Wostbrock [35]*). Granted,  $\Delta^{17}\text{O}$  discrepancies across laboratories and analytical techniques are not solved yet, but they should be tractable if addressed openly and in a collaborative manner.

In this study, we present new observations constraining  $\Delta^{17}\text{O}$  values of international carbonate standards relative to each other and, with a constant offset dictated by the fractionation parameters governing water- $\text{CO}_2$  equilibration and phosphoric acid reactions, relative to VSMOW/SLAP. These new measurements stand out in two distinct ways. For one thing, they were made using a spectroscopic technique specifically designed to optimize metrological precision and linearity in several ways (near-infra-red spectral region, low pressure conditions simplifying absorption line profiles, use of CRDS over direct absorption methods). The results reported in the first part of this study demonstrate that we achieve an instrumental precision of 0.004 ‰ on  $\Delta^{17}\text{O}$  in under 10 minutes, and that instrumental nonlinearities (pressure effects;  $\delta^{13}\text{C}$  effects, quadratic nonlinearities in  $\Delta^{17}\text{O}$ ) remain well below this threshold. Although working with  $\text{CO}_2$  analytes presents its own set of challenges and limitations, one potentially overlooked advantage of analyzing carbonates and waters converted to or equilibrated with  $\text{CO}_2$  is that when doing so, unknown analytes can then be bracketed in  $\delta^{18}\text{O}$  and  $\delta^{17}\text{O}$  by standards directly derived from VSMOW2 and SLAP2, which is not the case when analyzing total oxygen content. We thus believe that the data presented here will contribute usefully to the ongoing debate on triple oxygen isotope metrology.

Beyond oxygen-17 anomalies, future VCOF-CRDS developments will naturally focus on clumped-isotope measurements ( $\Delta_{638}$ ,  $\Delta_{828}$ ). Achieving the required sensitivity levels may prove challenging, but clumped-isotope measurements, being particularly sensitive to small instrumental non-linearities, would greatly benefit from the metrological qualities of VCOF-CRDS instruments. What's more, quasi-instantaneous switching from one diode to another potentially allows for measuring arbitrary combinations of  $\delta^{13}\text{C}$ ,  $\delta^{18}\text{O}$ ,  $\Delta^{17}\text{O}$ ,  $\Delta_{638}$ , and  $\Delta_{828}$  on relatively small amounts of  $\text{CO}_2$  using a single, high-throughput instrument, opening up many new applications.

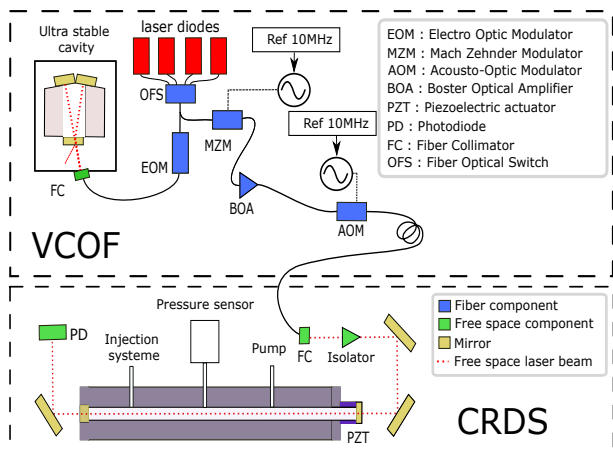


Figure 14 – Schematic of the VCOF-CRDS instrument. The spectrometer is based on two coupled systems. In the upper panel is the VCOF component, comprising laser diodes, a V-shaped stabilization cavity and the frequency tuning system. The CRDS cell (lower panel) is placed in a thermally regulated box. Modified from *Chaillot et al.* [41].

## Appendix

### A Brief technical overview of VCOF-CRDS

VCOF-CRDS is based on cavity ring-down measurements similar to those performed by widely used commercial instruments, but achieves superior metrological performances by locking a custom DFB fibered diode to a V-shaped optical cavity by optical feedback. An original feature of our setup is its ability to switch rapidly ( $\sim 1$  ms) between two fibered laser diodes, allowing us to target optimal absorption lines for each isotopologue. Further tunability is provided by a Mach-Zehnder Modulator (MZM) which subtracts a radio frequency component (RF) to the VCOF-locked optical frequency of the laser diode [62], with the RF being provided by a microwave synthesizer referenced to a GPS clock signal.

The frequency-shifted output of the MZM is injected in the CRDS cavity, whose length is adjusted using a piezoelectric actuator to keep the cavity mode resonant with the injected optical frequency. The optical power transmitted by the cavity increases as photons accumulate between the mirrors. When this transmitted power, detected by a photodiode, reaches a given threshold the light source is abruptly interrupted by an acousto-optic modulator (AOM). A ring-down (RD) event, i.e. the exponential decay of the photons circulating in the cavity, is then observed on the photodiode. The total optical loss  $\alpha_{\text{total}}$  of the cavity at this wavelength (not to be confused with an isotopic fractionation factor, despite using the same  $\alpha$  notation), which is the sum of mirror losses  $\alpha_{\text{mirror}}$  and gas absorption  $\alpha_{\text{gas}}$ , is deduced from the ring-down time constant ( $\tau$ ) and the speed of the light in vacuum ( $c$ ):

$$\alpha_{\text{total}} = \alpha_{\text{mirror}} + \alpha_{\text{gas}} = 1/\tau c \quad (11)$$

The mirror losses thus manifest as a slowly varying spectrum baseline on top of which sharp structures rise, corresponding to molecular absorption lines (fig. 15).

#### A.1 Ring-down acquisitions

In order to limit the impact of nonlinearities related to optical saturation [63] and/or photodiode transient response, the exponential fitting excludes the early part of the signal and only considers signal below 80 % of the threshold value. The stability and linearity of our acquisition hardware was assessed by measuring synthetic exponentials generated by a low noise, highly linear electronic circuit referenced to a GPS clock. Based on these experiments, systematic errors on  $\alpha_{\text{total}}$  introduced by our acquisition pipeline are two orders of magnitude below the random noise from the photodiode's shot noise limit ( $2\text{--}5 \cdot 10^{-12} \text{ cm}^{-1}$ ) [62].

For each wavelength, several  $\tau$  values are averaged. RD events are repeated every 5 ms, about 20 times the typical  $\tau$  value of 250  $\mu\text{s}$ . The number of RDs to be averaged is chosen according to the effective absorption coefficient at this wavelength. Typically, only 30 RDs are acquired on the baseline, but up to 250 are averaged for stronger absorption coefficients. This compensates for the increase of shot-to-shot noise as  $\tau$  decreases, allowing for constant measurement noise levels of  $\sim 5 \cdot 10^{-13} \text{ cm}^{-1}$ .

## A.2 Absorption coefficient measurements

Estimating isotopologue abundances from molecular absorption spectra is based on the physical property that the integrated area under each absorption peak is proportional, at a given temperature, to the partial pressure of the absorbing species. Absorption features are thus often recorded at high resolution over a broad spectral region. A spectroscopic model of absorption line shapes is then fitted to this observed spectrum to estimate the area under each absorption line profile [e.g., 25].

In practice, we found this approach to be sub-optimal when using VCOF-CRDS. For one thing, even state-of-the-art spectroscopic models using for instance Hartmann-Tran spectral line profiles [64, 65] do not reach the signal-to-noise level achieved with VCOF-CRDS [41]. Secondly, a technical limitation comes from the time required to record a single well-resolved spectrum, on the order of one minute. Over this time scale, isotopologue partial pressures vary slowly but detectably due to desorption/adsorption processes.

Faced with these limitations, we use an alternative, “parking” approach, whereby we sequentially sample the spectrum only near the top of a few isolated lines (B, C, D in fig. 15) and on the absorption baseline (A, E in fig. 15). After a short time ( $<10 \text{ s}$ ) spent measuring ABCDE in rapid sequence, we select a different laser diode, using a fast optical switch, to probe different isotopologues in another spectral region. In this study, we measure  $\delta^{13}\text{C}$ ,  $\delta^{18}\text{O}$  and  $\delta^{17}\text{O}$  by repeatedly alternating between two spectral regions (near 6231 and 6307  $\text{cm}^{-1}$ ) during 8 minutes.

## A.3 Data processing

The procedure by which we compute relative isotopologue abundances from absorption coefficient measurements is described below. In short, the partial pressure of each species is determined from baseline-corrected peak heights, with linear corrections for pressure broadening and no correction for potential cross-talk between isotopologues. These first-order assumptions are justifiable a priori because sample pressure is low, which limits line broadening/overlapping, and validated a posteriori by the experiments reported here.

The parking method yields an extremely sparse spectrum. Its accuracy thus derives from the extreme stability of our laser source (VCOF), implying that observed variations in the absorption coefficients

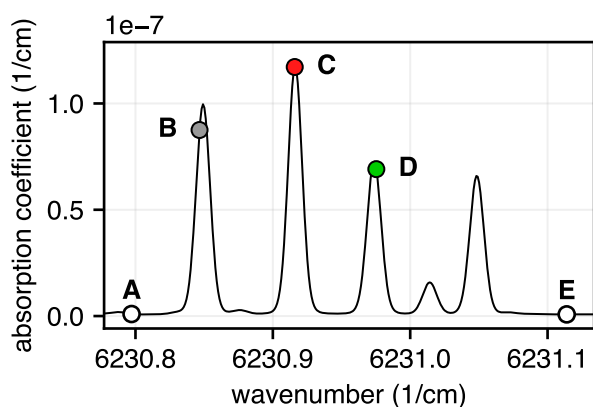


Figure 15 – Simulated  $\text{CO}_2$  absorption spectrum, in the region where our instruments measure the relative abundance of 626 (B), 628 (C) and 636 (D). The spectrum’s baseline is approximated by (AE).

reflect changes in isotopologue partial pressures rather than wavelength drift. Assuming constant temperature and total pressure in the measurement cell, each line profile should remain homothetic to the partial pressure of the corresponding species at any given wavelength, even away from the line center. Let us consider the points A, B, C, D, E of fig. 15, respectively sampled at wavelengths  $\nu_A, \dots, \nu_E$ . The gas absorption coefficients  $\alpha_B, \alpha_C, \alpha_D$  are determined from the measured total losses  $L_B, L_C, L_D$ , to which a baseline function  $BL(\nu)$ , assumed to be linear, must be subtracted. The baseline expression and gas absorption coefficients thus read:

$$\begin{aligned}
 BL(\nu) &= A_A + \frac{\nu - \nu_A}{\nu_E - \nu_A} (A_E - A_A) \\
 \alpha_B &= A_B - BL(\nu_B) \\
 \alpha_C &= A_C - BL(\nu_C) \\
 \alpha_D &= A_D - BL(\nu_D)
 \end{aligned} \tag{12}$$

The conversion from  $\alpha$  values to isotopologue partial pressures is calibrated once using pure  $\text{CO}_2$  of known pressure (and somewhat arbitrarily assumed isotopic composition), in steady-state continuous flow mode to eliminate contaminant outgassing and adsorption/desorption fluxes.

During “static” measurement on a finite amount of sample gas, however, the pressure varies slowly but continuously because of cell adsorption/desorption, and each measurement is done at a slightly different pressure due to the limited repeatability of the filling procedure ( $\pm 0.01$  mbar). As a result, each line shape is no longer homothetic to the partial pressure due to pressure broadening associated with the change of collisional environment, introducing the need for a pressure correction. This pressure correction, which was calibrated experimentally by a series of continuous flow measurements, using pure  $\text{CO}_2$  at pressures ranging well beyond the operational range of working pressures ( $\pm 2$  mbar), is a purely spectroscopic correction, which is not expected to vary over time.

The working-gas delta values ( $\delta_{627}, \delta_{628}, \delta_{636}$ ) obtained in the previous step are finally converted to ( $\delta^{17}\text{O}_{\text{VSMOW}}, \delta^{18}\text{O}_{\text{VSMOW}}, \delta^{13}\text{C}_{\text{VPDB}}$ ) values following the principle of two-anchor normalization [30, 36, 66], based either on  $\text{CO}_2$  equilibrated with water standards or on  $\text{CO}_2$  produced from acid digestion of carbonate standards. This standardization step, whose implementation is detailed in Appendix B, also yields analytical error estimates accounting for the observed repeatability of measurements, the number of replicate analyses for each sample, and additional uncertainties arising from the standardization itself.

## B Standardization procedure

### B.1 Standardization of $\delta^{13}\text{C}$

Using the method described above, each analysis yields a triplet of working-gas (WG) delta values ( $\delta_{636}$ ,  $\delta_{628}$ ,  $\delta_{627}$ ). To convert these WG-specific  $\delta_{636}$  values to  $\delta^{13}\text{C}$  in the VPDB scale, we use a least-squares minimization procedure inspired by the pooled regression approach proposed by *Daëron* [67] in the context of  $\Delta_{47}$  standardization. We start by dividing our analyses into “sessions”, i.e. finite time intervals during which analytical conditions are presumed to have remained stable. We then apply least-squares regression of a generative model predicting the WG-delta values. The model postulates that the  $\delta_{636}$  values measured in a given session are linked to the true  $^{13}\text{C}/^{12}\text{C}$  ratios of the analyte ( $x$ ) and working gas ( $wg$ ) by the following equation:

$$1 + \delta_{636}^x = f \cdot {}^{13}\text{R}^x / {}^{13}\text{R}^{wg} \quad (f \approx 1) \quad (13)$$

The true values of  ${}^{13}\text{R}^{wg}$  and  $f$  are unknown a priori and may vary from one session to another. Unless the analyte is a standard of known composition, the true value of  ${}^{13}\text{R}^x$  is also unknown, but it is assumed not to vary between sessions. The regression model parameters are thus (a) the true  $\delta^{13}\text{C}_{\text{VPDB}}$  value of each unknown  $\text{CO}_2$  sample; (b) the true  $\delta^{13}\text{C}_{\text{VPDB}}$  values of the WG used in each session, and (c) the scaling factor  $f$  describing scale compression or expansion within each session. This model is fit by searching for the combination of these parameters which minimizes the following  $\chi^2$  statistic over all analyses in a multi-session data set:

$$\sum \left( 1 + \delta_{636} - f \cdot \frac{1 + \delta^{13}\text{C}_{\text{VPDB}}^x}{1 + \delta^{13}\text{C}_{\text{VPDB}}^{wg}} \right)^2 \quad (14)$$

In the above equation,  $\delta_{636}$  is the measured value for each analysis;  $f$  and  $\delta^{13}\text{C}_{\text{VPDB}}^{wg}$  of the WG depend on the session; for unknown samples,  $\delta^{13}\text{C}_{\text{VPDB}}^x$  is one of the model parameters, whereas it is known a priori for “anchor” samples such as international and/or in-house reference materials.

Using such a pooled regression model rather than fitting each session separately avoids throwing away some useful information, because the distribution of  $\delta_{636}$  values for a given group of samples is preserved from one session to another through affine transformations. This approach does not substantially improve the apparent analytical precision, but it is more robust to outliers and properly accounts for uncertainties arising from standardization [67].

The above  $\chi^2$  formula is not scaled by uncertainties, implying that each analysis is assigned an equal weight in the regression. The final model variance is computed from the whole population of  $\delta_{636}$  residuals, and this variance is used to scale the covariance matrix of the best-fit parameters, including the best-fit estimates of  $\delta^{13}\text{C}_{\text{VPDB}}$  for all unknown samples. This covariance matrix thus characterizes the analytical errors (SE) for each sample as well as the correlations among these errors, and these error estimates fully account for (a) the overall repeatability of measurements, (b) the number of replicate analyses for each sample, and (c) additional analytical uncertainties arising from standardization.

Figure 16 provides a simple example of our standardization approach, with a simulated data set comprising two standards and two unknown samples, analyzed over two different sessions. In practice, the session-specific scaling factors for all of our VCOF-CRDS measurements remain within  $1.00 \pm 0.01$ . These values close to one are a foreseeable consequence of our parking strategy, which uses first-order approximations discussed in A.3.



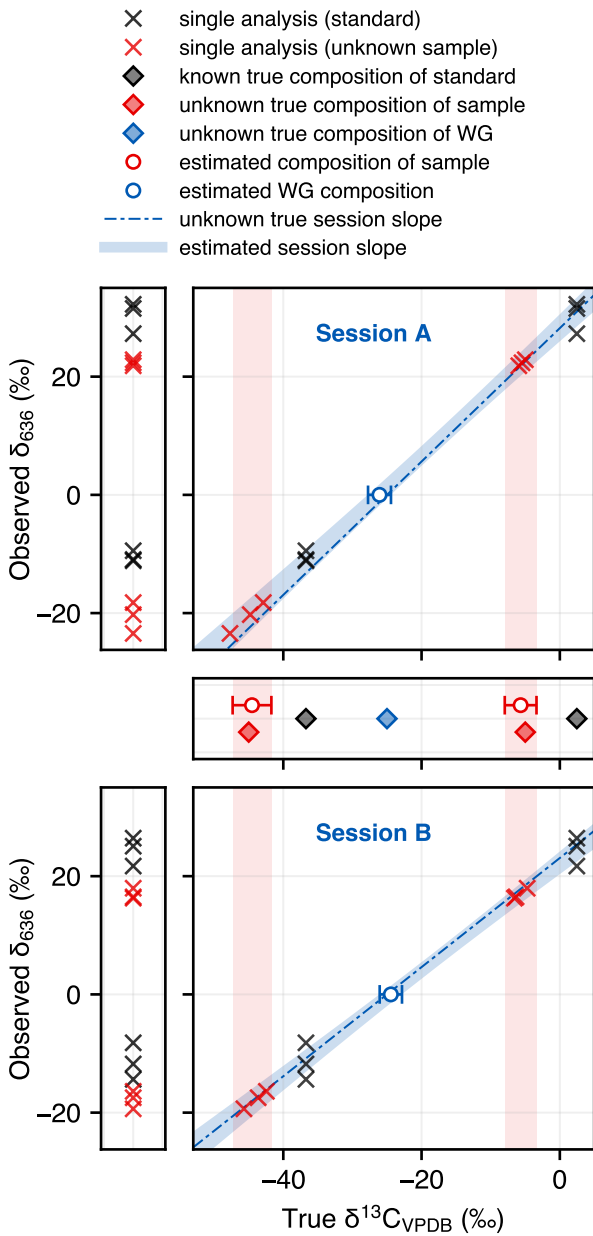


Figure 16 – Synthetic data set illustrating our standardization approach. Each standard (in black) and unknown sample (in red) were analyzed three times over two different sessions, yielding the  $\delta_{636}$  measurements shown in the left-most vertical panels. Standardizing this data set based on the known standard compositions is done by performing a joint least-squares optimization of the session parameters ( $f$  slope and WG composition, in blue) and sample compositions (in red) yields best-fit values. This statistically robust approach assigning equal weights to all analysis is conceptually identical to a two-anchor normalization [66]). The ordinarily unknown true compositions used to generate this data set are shown in the middle panel as blue and red diamonds. The scatter in  $\delta_{636}$  observations and variability of  $f$  values are greatly exaggerated for illustrative purposes.

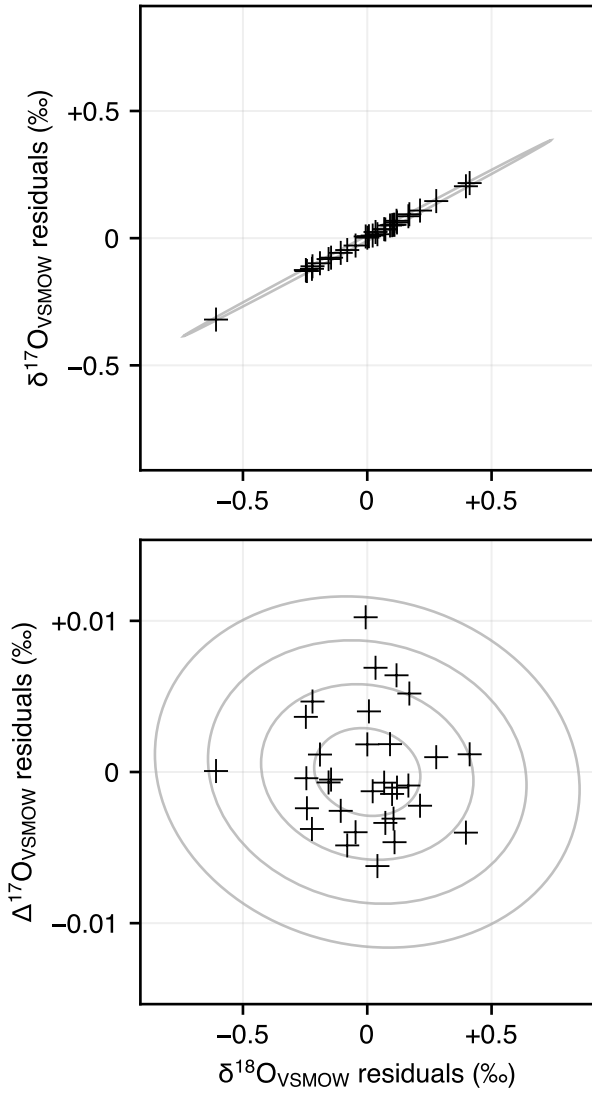


Figure 17 – Standardization residuals for the mixed water experiment of section 3.2.1. Each black cross corresponds to one analysis. Grey contours in the lower panel correspond to Mahalanobis distances of 1,2,3 and 4, i.e. to the 1-sigma, 2-sigma, 3-sigma and 4-sigma coverage ellipses based on the Minimum Covariance Determinant estimator. In the upper panel, only the 4-sigma contour is shown.

## B.2 Standardization of $\delta^{18}\text{O}$ and $\Delta^{17}\text{O}$

Standardization of  $\delta_{628}$  to  $\delta^{18}\text{O}$  values in the VSMOW-SLAP and/or VPDB scales is done in the same way as  $\delta^{13}\text{C}$ , but using different standards, such as  $\text{CO}_2$  equilibrated with water reference materials or produced by phosphoric acid digestion of carbonate standards (see below).

In theory, one could standardize  $\delta_{628}$  to  $\delta^{18}\text{O}$  and  $\delta_{627}$  to  $\delta^{17}\text{O}$  independently, but this would amount to performing two statistically independent regressions on separate data sets, yielding mathematically independent uncertainties on final  $\delta^{18}\text{O}$  and  $\delta^{17}\text{O}$  values on the order of 0.1–0.2 ‰, and thus unacceptably large  $\Delta^{17}\text{O}$  uncertainties.

In reality, the regression residuals on  $\delta_{628}$  and  $\delta_{627}$  values are not independent but strongly correlated, with a slope close to 0.528, so that  $\Delta^{17}\text{O}$  repeatability is an order of magnitude better than 0.1 ‰ (fig. 17). To model this behavior, we propose a modified standardization procedure where the model parameters are (a) the true  $\delta^{18}\text{O}_{\text{VSMOW}}$  and  $\Delta^{17}\text{O}_{\text{VSMOW}}$  values of each unknown  $\text{CO}_2$  sample; (b) the true  $\delta^{18}\text{O}_{\text{VSMOW}}$  and  $\Delta^{17}\text{O}_{\text{VSMOW}}$  values of the WG used in each session, and (c) session-specific scaling factors  $f_{627}$  and  $f_{628}$  characterizing, as before, scale compression or expansion between  $\delta^{18}\text{O}_{\text{VSMOW}}$  and  $\delta_{628}$  values and between  $\delta^{17}\text{O}_{\text{VSMOW}}$  and  $\delta_{627}$  values.

The regression residuals for  $n$  measurements are a set of  $n$  vectors, either in  $(\delta_{628}, \delta_{627})$  or in  $(\delta_{628}, \Delta^{17}\text{O}_{\text{WG}})$  space. The distribution of these residuals may be summarized by applying a statistically robust covariance estimator such as the Minimum Covariance Determinant [68], yielding a 2-by-2 covariance matrix CM. The  $\chi^2$  statistic we then attempt to minimize is the sum of squared Mahalanobis distances between the residual vectors and the two-dimensional distribution defined by CM:

$$\sum (r_{628}, r_{627}) \cdot \text{CM}^{-1} \cdot (r_{628}, r_{627})^{\top} \quad (15)$$

where where  $r_{628}$  are the  $\delta_{628}$  model residuals, and  $r_{627}$  the  $\delta_{627}$  (or  $\Delta^{17}\text{O}_{\text{WG}}$ ) residuals. In practice, the choice to express 627 residuals in terms of  $\delta_{627}$  or  $\Delta^{17}\text{O}_{\text{WG}}$  has no influence (at the 0.0001 ‰ level) on final results. By using the Mahalanobis distance, we are effectively scaling the contribution of 628 and 627 residuals by their respective sample variances and properly accounting for the observed (instead of assumed) correlation between 628 and 628 residuals [69]. In the end, this joint regression procedure once again yields best-fit estimates for the  $\delta^{18}\text{O}$  and  $\Delta^{17}\text{O}$  values of each unknown sample, along with all corresponding analytical standard errors and their correlations.

An open-source implementation of the standardization methods described above is available as a Python library (`stdz.py`) in the code and data repository associated with this study (see below).

## Acknowledgements

The work reported here received support from the following institutions: Agence Nationale de la Recherche (JCJC), Institut National des Sciences de l'Univers (LEFE), Centre National de la Recherche Scientifique (MITI), Région Ile-de-France (SESAME, DIM PAMIR), Commissariat à l'Energie Atomique et aux Energies Alternatives, Université de Versailles St-Quentin-en-Yvelines, and Université Paris-Saclay, the IAEA Collaborating Centre "Atoms for Heritage", and REFIMEVE+. This work benefitted in many ways from the stimulating discussions we had over the years with J. Burkart, E. Kerstel, D. Romanini, T. Stoltmann, A. Campargue, H. Fleurbaey, and J. Savarino. We are grateful for the insightful comments of three anonymous reviewers and for D. Porcelli's editorial handling. We thank S. Assonov for pointing us to the earlier measurements of IAEA610/611/612 performed at HUJ and E. Barkan, H. Affek for graciously sharing these results.

## Author contributions

Conceptualization and funding: MD, SK, AL; instrumental development: JC, SK, MC, MD; spectroscopic methodology: SK, MC experimental design: MD; sample preparation: TC, MP, MD; analyses: JC, SK, TC, MP; data validation: JC, TC, MP; data processing: SK, MD; reproducible source code: MD; IRMS measurements: AL; manuscript drafting: JC, MD; manuscript revision: all co-authors.

## Reproducible research

The complete data set and code base for this study are archived at Zenodo under a MIT license (<https://doi.org/10.5281/zenodo.14007201>). The preferred way to comment on the code or to suggest improvements is to raise an issue at <https://github.com/mdaeron/RM-17O-by-VCOF-CRDS>.

## References

- [1] H. Craig. Isotopic standards for carbon and oxygen and correction factors for mass spectrometric analysis of carbon dioxide. *Geochimica et Cosmochimica Acta* 12 (1957), pp. 133–149.
- [2] M. F. Miller & A. Pack. Why Measure  $^{17}\text{O}$ ? Historical Perspective, Triple-Isotope Systematics and Selected Applications. *Reviews in Mineralogy and Geochemistry* 86:(1) (2021), pp. 1–34.
- [3] B. H. Passey, H. Hu, H. Ji, S. Montanari, S. Li, G. A. Henkes, & N. E. Levin. Triple oxygen isotopes in biogenic and sedimentary carbonates. *Geochimica et Cosmochimica Acta* 141 (2014), pp. 1–25.
- [4] S. J. Bergel, E. Barkan, M. Stein, & H. P. Affek. Carbonate  $^{17}\text{O}_{\text{excess}}$  as a paleo-hydrology proxy: Triple oxygen isotope fractionation between  $\text{H}_2\text{O}$  and biogenic aragonite, derived from freshwater mollusks. *Geochimica et Cosmochimica Acta* 275 (2020), pp. 36–47.
- [5] J. A. G. Wostbrock, U. Brand, T. B. Coplen, P. K. Swart, S. J. Carlson, A. J. Brearley, & Z. D. Sharp. Calibration of carbonate-water triple oxygen isotope fractionation: Seeing through diagenesis in ancient carbonates. *Geochimica et Cosmochimica Acta* 288 (2020), pp. 369–388.
- [6] D. Herwartz. Triple Oxygen Isotope Variations in Earth's Crust. *Reviews in Mineralogy and Geochemistry* 86:(1) (2021), pp. 291–322.
- [7] B. H. Passey & N. E. Levin. Triple Oxygen Isotopes in Meteoric Waters, Carbonates, and Biological Apatites: Implications for Continental Paleoclimate Reconstruction. *Reviews in Mineralogy and Geochemistry* 86:(1) (2021), pp. 429–462.
- [8] J. R. Kelson, S. V. Petersen, N. A. Niemi, B. H. Passey, & A. N. Curley. Looking upstream with clumped and triple oxygen isotopes of estuarine oyster shells in the early Eocene of California, USA. *Geology* 50:(7) (2022), pp. 755–759.
- [9] T. E. Huth, B. H. Passey, J. E. Cole, M. S. Lachniet, D. McGee, R. F. Denniston, S. Truebe, & N. E. Levin. A framework for triple oxygen isotopes in speleothem paleoclimatology. *Geochimica et Cosmochimica Acta* 319 (2022), pp. 191–219.
- [10] T. Sharma & R. N. Clayton. Measurement of ratios of total oxygen of carbonates. *Geochimica et Cosmochimica Acta* 29:(12) (1965), pp. 1347–1353.
- [11] S. K. Bhattacharya & M. H. Thiemens. Effect of Isotopic Exchange upon Symmetry Dependent Fractionation in the  $\text{O} + \text{CO} \rightarrow \text{CO}_2$  Reaction. *Zeitschrift für Naturforschung A* 44:(9) (1989), pp. 811–813.
- [12] J. A. G. Wostbrock, E. J. Cano, & Z. D. Sharp. An internally consistent triple oxygen isotope calibration of standards for silicates, carbonates and air relative to VSMOW2 and SLAP2. *Chemical Geology* 533 (2020), pp. 119432.
- [13] C. A. M. Brenninkmeijer & T. Röckmann. A rapid method for the preparation of  $\text{O}_2$  from  $\text{CO}_2$  for mass spectrometric measurement of  $^{17}\text{O}/^{16}\text{O}$  ratios. *Rapid Communications in Mass Spectrometry* 12:(8) (1998), pp. 479–483.
- [14] N. M. Ellis & B. H. Passey. A novel method for high-precision triple oxygen isotope analysis of diverse Earth materials using high temperature conversion–methanation–fluorination and isotope ratio mass spectrometry. *Chemical Geology* 635 (2023), pp. 121616.
- [15] S.S. Assonov & C. A. M. Brenninkmeijer. A new method to determine the  $^{17}\text{O}$  isotopic abundance in  $\text{CO}_2$  using oxygen isotope exchange with a solid oxide. *Rapid Communications in Mass Spectrometry* 15:(24) (2001), pp. 2426–2437.
- [16] S. Kawagucci, U. Tsunogai, S. Kudo, F. Nakagawa, H. Honda, S. Aoki, T. Nakazawa, & T. Gamo. An Analytical System for Determining  $\delta^{17}\text{O}$  in  $\text{CO}_2$  Using Continuous Flow-Isotope Ratio MS. *Analytical Chemistry* 77:(14) (2005), pp. 4509–4514.
- [17] M. E. G. Hofmann & A. Pack. Technique for High-Precision Analysis of Triple Oxygen Isotope Ratios in Carbon Dioxide. *Analytical Chemistry* 82:(11) (2010), pp. 4357–4361.
- [18] S. Mahata, S. K. Bhattacharya, C.-H. Wang, & M.-C. Liang. An improved  $\text{CeO}_2$  method for high-precision measurements of  $^{17}\text{O}/^{16}\text{O}$  ratios for atmospheric carbon dioxide. *Rapid Communications in Mass Spectrometry* 26:(17) (2012), pp. 1909–1922.
- [19] E. Barkan & B. Luz. High-precision measurements of  $^{17}\text{O}/^{16}\text{O}$  and  $^{18}\text{O}/^{16}\text{O}$  ratios in  $\text{CO}_2$ . *Rapid Communications in Mass Spectrometry* 26 (2012), pp. 2733–2738.
- [20] S. Mahata, S. K. Bhattacharya, C.-H. Wang, & M.-C. Liang. Oxygen Isotope Exchange between  $\text{O}_2$  and  $\text{CO}_2$  over Hot Platinum: An Innovative Technique for Measuring  $\Delta^{17}\text{O}$  in  $\text{CO}_2$ . *Analytical Chemistry* 85:(14) (2013), pp. 6894–6901.
- [21] A. Mahata, P. Bhauriyal, K. S. Rawat, & B. Pathak.  $\text{Pt}_3\text{Ti}$  ( $\text{Ti}_{19}\text{@Pt}_{60}$ )-Based Cuboctahedral Core–Shell Nanocluster Favors a Direct over Indirect Oxygen Reduction Reaction. *ACS Energy Letters* 1:(4) (2016), pp. 797–805.
- [22] F. Castiglione, A. Mele, & G. Raos.  $^{17}\text{O}$  NMR. *Annual Reports on NMR Spectroscopy*. Elsevier, 2015, p. 143–193.
- [23] G. A. Adnew, M. E. G. Hofmann, D. Paul, A. Laskar, J. Surma, N. Albrecht, A. Pack, J. Schwieters, G. Koren, W. Peters, & T. Röckmann. Determination of the triple oxygen and carbon isotopic composition of  $\text{CO}_2$  from atomic ion fragments formed in the ion source of the 253 Ultra High-Resolution Isotope Ratio Mass Spectrometer. *Rapid Communications in Mass Spectrometry* 33:(17) (2019), pp. 1363–1380.
- [24] D. Romanini, I. Ventrillard, G. Méjean, J. Morville, & E. Kerstel. Introduction to Cavity Enhanced Absorption Spectroscopy. *Cavity-Enhanced Spectroscopy and Sensing*. Edited by G. Gagliardi & H.-P. Loock. Volume 179. Berlin, Heidelberg: Springer Berlin Heidelberg, 2014, p. 1–60.
- [25] T. Stoltmann, M. Casado, M. Daëron, A. Landais, & S. Kassi. Direct, Precise Measurements of Isotopologue Abundance Ratios in  $\text{CO}_2$  Using Molecular Absorption Spectroscopy: Application to  $\Delta^{17}\text{O}$ . *Analytical Chemistry* 89:(19) (2017), pp. 10129–10132.

- [26] N. Yanay, Z. Wang, D. L. Dettman, J. Quade, K. W. Huntington, A. J. Schauer, D. D. Nelson, J. B. McManus, K. Thirumalai, S. Sakai, A. Rebaza Morillo, & A. Mallik. Rapid and precise measurement of carbonate clumped isotopes using laser spectroscopy. *Science Advances* 8:(43) (2022).
- [27] V. J. Hare, C. Dyroff, D. D. Nelson, & D. A. Yarian. High-Precision Triple Oxygen Isotope Analysis of Carbon Dioxide by Tunable Infrared Laser Absorption Spectroscopy. *Analytical Chemistry* 94:(46) (2022), pp. 16023–16032.
- [28] N. Perdue, Z. Sharp, D. Nelson, R. Wehr, & C. Dyroff. A rapid high-precision analytical method for triple oxygen isotope analysis of CO<sub>2</sub> gas using tunable infrared laser direct absorption spectroscopy. *Rapid Communications in Mass Spectrometry* 36:(21) (2022).
- [29] T. B. Coplen, C. Kendall, & J. Hopple. Comparison of stable isotope reference samples. *Nature* 302:(5905) (1983), pp. 236–238. [10.1038/302236a0](https://doi.org/10.1038/302236a0).
- [30] S.-T. Kim, T. B. Coplen, & J. Horita. Normalization of stable isotope data for carbonate minerals: Implementation of IUPAC guidelines. *Geochimica et Cosmochimica Acta* 158 (2015), pp. 276–289.
- [31] R. A. Werner & W. A. Brand. Referencing strategies and techniques in stable isotope ratio analysis. *Rapid Communications in Mass Spectrometry* 15:(7) (2001), pp. 501–519. [10.1002/rcm.258](https://doi.org/10.1002/rcm.258).
- [32] E. Barkan, I. Musan, & B. Luz. High-precision measurements of  $\delta^{17}\text{O}$  and  $^{17}\text{O}_{\text{excess}}$  of NBS19 and NBS18. *Rapid Communications in Mass Spectrometry* 29 (2015), pp. 2219–2224.
- [33] B. H. Passey & H. Ji. Triple oxygen isotope signatures of evaporation in lake waters and carbonates: A case study from the western United States. *Earth and Planetary Science Letters* 518 (2019), pp. 1–12.
- [34] B. R. Fosu, R. Subba, R. Peethambaran, S. K. Bhattacharya, & P. Ghosh. Technical Note: Developments and Applications in Triple Oxygen Isotope Analysis of Carbonates. *ACS Earth and Space Chemistry* 4:(5) (2020), pp. 702–710.
- [35] Z. D. Sharp & J. A. G. Wostbrock. Standardization for the Triple Oxygen Isotope System: Waters, Silicates, Carbonates, Air, and Sulfates. *Reviews in Mineralogy and Geochemistry* 86:(1) (2021), pp. 179–196.
- [36] C. Hillaire-Marcel, S.-T. Kim, A. Landais, P. Ghosh, S. Assonov, C. Lécuyer, M. Blanchard, H. A. J. Meijer, & H. C. Steen-Larsen. A stable isotope toolbox for water and inorganic carbon cycle studies. *Nature Reviews Earth & Environment* 2:(10) (2021), pp. 699–719.
- [37] W. Guo & C. Zhou. Triple oxygen isotope fractionation in the DIC-H<sub>2</sub>O-CO<sub>2</sub> system: a numerical framework and its implications. *Geochimica et Cosmochimica Acta* 246 (2019), pp. 541–564.
- [38] I.E. Gordon, L.S. Rothman, R.J. Hargreaves, R. Hashemi, E.V. Karlovets, F.M. Skinner, E.K. Conway, C. Hill, R.V. Kochanov, Y. Tan, P. Wcisło, A.A. Finenko, K. Nelson, P.F. Bernath, M. Birk, V. Boudon, A. Campargue, K.V. Chance, A. Coustenis, B.J. Drouin, J.-M. Flaud, R.R. Gamache, J.T. Hodges, D. Jacquemart, E.J. Mlawer, A.V. Nikitin, V.I. Perevalov, M. Rotger, J. Tennyson, G.C. Toon, H. Tran, V.G. Tyuterev, E.M. Adkins, A. Baker, A. Barbe, E. Canè, A.G. Császár, A. Dudaryonok, O. Egorov, A.J. Fleisher, H. Fleurbaey, A. Foltynowicz, T. Furtenbacher, J.J. Harrison, J.-M. Hartmann, V.-M. Horneman, X. Huang, T. Karman, J. Karns, S. Kassi, I. Kleiner, V. Kofman, F. Kwabia-Tchana, N.N. Lavrentieva, T.J. Lee, D.A. Long, A.A. Lukashchanskaya, O.M. Lyulin, V.Yu. Makhnev, W. Matt, S.T. Massie, M. Melosso, S.N. Mikhailenko, D. Mondelain, H.S.P. Müller, O.V. Naumenko, A. Perrin, O.L. Polyansky, E. Raddaoui, P.L. Raston, Z.D. Reed, M. Rey, C. Richard, R. Tóbiás, I. Sadiq, D.W. Schwenke, E. Starikova, K. Sung, F. Tamassia, S.A. Tashkun, J. Vander Auwera, I.A. Vasilenko, A.A. Viganin, G.L. Villanueva, B. Vispoel, G. Wagner, A. Yachmenev, & S.N. Yurchenko. The HITRAN2020 molecular spectroscopic database. *Journal of Quantitative Spectroscopy and Radiative Transfer* 277 (2022), pp. 107949.
- [39] S.S. Assonov & C.A.M. Brenninkmeijer. On the  $^{17}\text{O}$  correction for CO<sub>2</sub> mass spectrometric isotopic analysis. *Rapid Communications in Mass Spectrometry* 17 (2003), pp. 1007–1016.
- [40] J. Burkart, D. Romanini, & S. Kassi. Optical feedback frequency stabilized cavity ring-down spectroscopy. *Optics Letters* 39:(16) (2014), pp. 4695.
- [41] J. Chaillot, S. Dasari, H. Fleurbaey, M. Daëron, J. Savarino, & S. Kassi. High-precision laser spectroscopy of H<sub>2</sub>S for simultaneous probing of multiple-sulfur isotopes. *Environmental Science: Advances* (2022).
- [42] M. Casado, T. Stoltmann, A. Landais, N. Jobert, M. Daëron, F. Prié, & S. Kassi. High stability in near-infrared spectroscopy: part 1, adapting clock techniques to optical feedback. *Applied Physics B* 128:(3) (2022).
- [43] L. Djehahirdjian, L. Lechevallier, M.-A. Martin-Drumel, O. Pirali, G. Ducournau, R. Kassi, & S. Kassi. Frequency stable and low phase noise THz synthesis for precision spectroscopy. *Nature Communications* 14:(1) (2023), pp. 7162.
- [44] D. Romanini, A. A. Kachanov, N. Sadeghi, & F. Stoekel. CW cavity ring down spectroscopy. *Chemical Physics Letters* 264:(3–4) (1997), pp. 316–322.
- [45] E. A. Atekwana, F. Meints, & R. V. Krishnamurthy. A versatile glass tube cracker for transfer of gases from sealed glass tubes for stable isotope ratio and chemical analyses. *Rapid Communications in Mass Spectrometry* 24:(21) (2010), pp. 3219–3220.
- [46] C. Vallet-Coulomb, M. Couapel, & C. Sonzogni. Improving memory effect correction to achieve high-precision analysis of  $\delta^{17}\text{O}$ ,  $\delta^{18}\text{O}$ ,  $\delta^2\text{H}$ ,  $^{17}\text{O}$ -excess and d-excess in water using cavity ring-down laser spectroscopy. *Rapid Communications in Mass Spectrometry* 35:(14) (2021), pp. e9108.
- [47] S. Epstein & T. Mayeda. Variation of O<sup>18</sup> content of waters from natural sources. *Geochimica et Cosmochimica Acta* 4:(5) (1953), pp. 213–224.
- [48] W. C. Beck, E. L. Grossman, & J. W. Morse. Experimental studies of oxygen isotope fractionation in the carbonic acid system at 15 °, 25 °, and 40 °C. *Geochimica et Cosmochimica Acta* 69:(14) (2005), pp. 3493–3503.

- [49] Sergey Assonov, Ales Fajgelj, Colin Allison, & Manfred Gröning. On the metrological traceability and hierarchy of stable isotope reference materials aimed at realisation of the VPDB scale: revision of the VPDB  $\delta_{13}\text{C}$  scale based on multipoint scale-anchoring RMs. *Rapid Communications in Mass Spectrometry* 35:(8) (2021).
- [50] J. Viallon, T. Choteau, E. Flores, F. Idrees, P. Moussay, R. I. Wielgosz, Z. Loh, C. Allison, L. Huang, A. Chivelscu, F. Camin, B. Krajnc, N. Ogrinc, A. de Lima Fioravante, M. Fasciotti, T. V. C. Monteiro, B. C. Garrido, E. C. P. Rego, W. Wollinger, C. R. Augusto, S. Michel, J. S. Lee, J. K. Lim, M. Daëron, S. Kassi, H. Moossen, L. Hai, Z. Zhou, A. Srivastava, T. Shimosaka, E. Mussel Webber, R. Hill-Pearce, P. Brewer, M. Chartrand, O. Rienitz, V. Ebert, L. Flierl, J. Braden-Behrens, J. Nwaboh, A. Emad, A. Simsek, & I. Chubchenko. Final report of CCQM-P204, comparison on  $\text{CO}_2$  isotope ratios in pure  $\text{CO}_2$ . *Metrologia* 60:(1A) (2023), pp. 08026.
- [51] W. A. Brand, S. S. Assonov, & T. B. Coplen. Correction for the  $^{17}\text{O}$  interference in  $\delta^{13}\text{C}$  measurements when analyzing  $\text{CO}_2$  with stable isotope mass spectrometry (IUPAC Technical Report). *Pure and Applied Chemistry* 82:(8) (2010), pp. 1719–1733.
- [52] L. Sha, S. Mahata, P. Duan, B. Luz, P. Zhang, J. Baker, B. Zong, Y. Ning, Y. A. Brahim, H. Zhang, R. L. Edwards, & H. Cheng. A novel application of triple oxygen isotope ratios of speleothems. *Geochimica et Cosmochimica Acta* 270 (2020), pp. 360–378.
- [53] E. Barkan, H. P. Affek, B. Luz, S. J. Bergel, N. R. G. Voarintsoa, & I. Musan. Calibration of  $\delta^{17}\text{O}$  and  $\delta^{17}\text{O}_{\text{excess}}$  values of three international standards: IAEA-603, NBS19 and NBS18. *Rapid Communications in Mass Spectrometry* 33:(7) (2019), pp. 737–740.
- [54] S. Assonov. Assessment of the accuracy of the  $^{17}\text{O}$  correction algorithm used in  $\delta^{13}\text{C}$  determinations by  $\text{CO}_2$  mass spectrometry. *Rapid Communications in Mass Spectrometry* 37:(9) (2023). [10.1002/rcm.9490](https://doi.org/10.1002/rcm.9490).
- [55] J. Fiebig, M. Bernecker, N. Meijer, K. Methner, P. T. Staudigel, A. J. Davies, L. Bayarjargal, D. Spahr, B. Winkler, S. Hofmann, M. Granzin, & S. V. Petersen. Carbonate clumped isotope values compromised by nitrate-derived  $\text{NO}_2$  interferent. *Chemical Geology* 670 (2024), pp. 122382. [10.1016/j.chemgeo.2024.122382](https://doi.org/10.1016/j.chemgeo.2024.122382).
- [56] S. F. Crowley. Mineralogical and Chemical Composition of International Carbon and Oxygen Isotope Calibration Material NBS 19, and Reference Materials NBS 18, IAEA-CO-1 and IAEA-CO-8. *Geostandards and Geoanalytical Research* 34:(2) (2010), pp. 193–206. [10.1111/j.1751-908x.2010.00037.x](https://doi.org/10.1111/j.1751-908x.2010.00037.x).
- [57] Y. Wei, H. Yan, Y. Peng, S. Han, & H. Bao. Thermal-gradient-induced isotope fractionation during  $\text{CO}_2$ - $\text{O}_2$  triple oxygen isotope exchange. *Geochimica et Cosmochimica Acta* 370 (2024), pp. 29–40. [10.1016/j.gca.2024.02.010](https://doi.org/10.1016/j.gca.2024.02.010).
- [58] K. J. Dennis, H. P. Affek, B. H. Passey, D. P. Schrag, & J. M. Eiler. Defining an absolute reference frame for ‘clumped’ isotope studies of  $\text{CO}_2$ . *Geochimica et Cosmochimica Acta* 75 (2011), pp. 7117–7131.
- [59] B. He, G. A. Olack, & A. S. Colman. Pressure baseline correction and high-precision  $\text{CO}_2$  clumped-isotope ( $\Delta_{47}$ ) measurements in bellows and micro-volume modes. *Rapid Communications in Mass Spectrometry* 26 (2012), pp. 2837–2853.
- [60] S. M. Bernasconi, B. Hu, U. Wacker, J. Fiebig, S. F. M. Breitenbach, & T. Rutz. Background effects on Faraday collectors in gas-source mass spectrometry and implications for clumped isotope measurements. *Rapid Communications in Mass Spectrometry* 27:(5) (2013), pp. 603–612.
- [61] L. Y. Yeung, J. A. Hayles, H. Hu, J. L. Ash, & T. Sun. Scale distortion from pressure baselines as a source of inaccuracy in triple-isotope measurements. *Rapid Communications in Mass Spectrometry* 32:(20) (2018), pp. 1811–1821.
- [62] J. Burkart, D. Romanini, & S. Kassi. Optical feedback stabilized laser tuned by single-sideband modulation. *Optics Letters* 38:(12) (2013), pp. 2062.
- [63] S. Kassi, T. Stoltmann, M. Casado, M. Daëron, & A. Campargue. Lamb dip CRDS of highly saturated transitions of water near  $1.4\ \mu\text{m}$ . *The Journal of Chemical Physics* 148:(5) (2018), pp. 054201.
- [64] N.H. Ngo, D. Lisak, H. Tran, & J.-M. Hartmann. An isolated line-shape model to go beyond the Voigt profile in spectroscopic databases and radiative transfer codes. *Journal of Quantitative Spectroscopy and Radiative Transfer* 129 (2013), pp. 89–100.
- [65] J.-M. Hartmann, C. Boulet, & D. Robert. *Collisional effects on molecular spectra: laboratory experiments and models, consequences for applications*. Second edition. Amsterdam Oxford Cambridge, MA: Elsevier, 2021.
- [66] T. B. Coplen, P. De Bièvre, H. R. Krouse, R. D. Vocke, M. Gröning, & K. Rozanski. Ratios for light-element isotopes standardized for better interlaboratory comparison. *Eos, Transactions American Geophysical Union* 77:(27) (1996), pp. 255–255.
- [67] M. Daëron. Full propagation of analytical uncertainties in  $\Delta_{47}$  measurements. *Geochemistry, Geophysics, Geosystems* 22:(5) (2021).
- [68] P. J. Rousseeuw. Least Median of Squares Regression. *Journal of the American Statistical Association* 79:(388) (1984), pp. 871–880.
- [69] R. De Maesschalck, D. Jouan-Rimbaud, & D. L. Massart. The Mahalanobis distance. *Chemometrics and Intelligent Laboratory Systems* 50:(1) (2000), pp. 1–18.